

**High-pressure electrochemical reduction of CO₂ to formic acid/formate
Effect of pH on the downstream separation process and economics**

Ramdin, Mahinder; Morrison, Andrew R.T.; De Groen, Mariette; Van Haperen, Rien; De Kler, Robert; Irtem, Erdem; Laitinen, Antero T.; Van Den Broeke, Leo J.P.; Breugelmans, Tom; Trusler, J. P. Martin

DOI

[10.1021/acs.iecr.9b03970](https://doi.org/10.1021/acs.iecr.9b03970)

Publication date

2019

Document Version

Final published version

Published in

Industrial and Engineering Chemistry Research

Citation (APA)

Ramdin, M., Morrison, A. R. T., De Groen, M., Van Haperen, R., De Kler, R., Irtem, E., Laitinen, A. T., Van Den Broeke, L. J. P., Breugelmans, T., Trusler, J. P. M., Jong, W. D., & Vlugt, T. J. H. (2019). High-pressure electrochemical reduction of CO₂ to formic acid/formate: Effect of pH on the downstream separation process and economics. *Industrial and Engineering Chemistry Research*, 58(51), 22718-22740. <https://doi.org/10.1021/acs.iecr.9b03970>

Important note

To cite this publication, please use the final published version (if applicable).
Please check the document version above.

Copyright

Other than for strictly personal use, it is not permitted to download, forward or distribute the text or part of it, without the consent of the author(s) and/or copyright holder(s), unless the work is under an open content license such as Creative Commons.

Takedown policy

Please contact us and provide details if you believe this document breaches copyrights.
We will remove access to the work immediately and investigate your claim.

High-Pressure Electrochemical Reduction of CO₂ to Formic Acid/Formate: Effect of pH on the Downstream Separation Process and Economics

Mahinder Ramdin,[†] Andrew R. T. Morrison,[‡] Mariette de Groen,[§] Rien van Haperen,[§] Robert de Kler,[§] Erdem Irtem,^{||} Antero T. Laitinen,[⊥] Leo J. P. van den Broeke,[†] Tom Breugelmans,^{||} J. P. Martin Trusler,[#] Wiebren de Jong,[‡] and Thijs J. H. Vlugt^{*,†}

[†]Engineering Thermodynamics, Process & Energy Department, Faculty of Mechanical, Maritime and Materials Engineering and

[‡]Large-Scale Energy Storage, Process & Energy Department, Faculty of Mechanical, Maritime and Materials Engineering, Delft University of Technology, Leeghwaterstraat 39, 2628CB Delft, The Netherlands

[§]Coval Energy, Wilhelminasingel 14, 4818AA Breda, The Netherlands

^{||}Research Group Advanced Reactor Technology, University of Antwerp, Universiteitsplein 1, B-2610 Wilrijk, Belgium

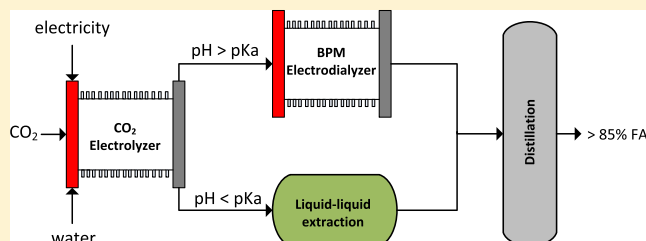
[⊥]VTT Technical Research Centre of Finland, Tietotie 4 E, 02150 Espoo, Finland

[#]Imperial College London, South Kensington Campus, London SW7 2AZ, United Kingdom

Supporting Information

ABSTRACT: We use a high-pressure semicontinuous batch electrochemical reactor with a tin-based cathode to demonstrate that it is possible to efficiently convert CO₂ to formic acid (FA) in low-pH (i.e., pH < pK_a) electrolyte solutions. The effects of CO₂ pressure (up to 50 bar), bipolar membranes, and electrolyte (K₂SO₄) concentration on the current density (CD) and the Faraday efficiency (FE) of formic acid were investigated. The highest FE (~80%) of FA was achieved at a pressure of around 50 bar at a cell potential of 3.5 V and a CD of ~30 mA/cm².

To suppress the hydrogen evolution reaction (HER), the electrochemical reduction of CO₂ in aqueous media is typically performed at alkaline conditions. The consequence of this is that products like formic acid, which has a pK_a of 3.75, will almost completely dissociate into the formate form. The pH of the electrolyte solution has a strong influence not only on the electrochemical reduction process of CO₂ but also on the downstream separation of (dilute) acid products like formic acid. The selection of separation processes depends on the dissociation state of the acids. A review of separation technologies for formic acid/formate removal from aqueous dilute streams is provided. By applying common separation heuristics, we have selected liquid–liquid extraction and electro dialysis for formic acid and formate separation, respectively. An economic evaluation of both separation processes shows that the formic acid route is more attractive than the formate one. These results urge for a better design of (1) CO₂ electrocatalysts that can operate at low pH without affecting the selectivity of the desired products and (2) technologies for efficient separation of dilute products from (photo)electrochemical reactors.



INTRODUCTION

Carbon capture and utilization (CCU) has been proposed as a complementary measure to mitigate CO₂ emissions. An interesting example of CCU is the electrochemical conversion of CO₂ to chemicals and fuels using renewable electricity (i.e., power-to-X).^{1,2} Currently, it is very challenging for electrochemical processes to compete with the fossil-fuel-based counterparts in the chemical industry.^{3,4} Nevertheless, a tremendous effort was made in the last decade to improve the performance metrics of the CO₂ reduction reaction (CRR), i.e., the Faraday efficiency (FE, the product selectivity), the current density (CD, the reaction rate), and the overpotential (the excess potential to drive the reaction).^{5–10} The complexity lies in the fact that the CRR is influenced by many factors, i.e., the

type and morphology of the catalyst, temperature, pressure, pH, type and concentration of electrolytes, type of solvent, flow characteristics, type of membranes, impurities, type of electrode (flat, porous, gas diffusion), etc.^{11–16} So far, only the two electron CO₂ reduction products carbon monoxide (CO) and formic acid/formate (FA/HCOO[−]) have been produced with a high FE (>90%) and CD (>100 mA/cm²) but at a lab scale. Note that formic acid is a hydrogen and CO carrier, which can play an important role in energy storage.¹⁷ A gross-margin

Received: July 19, 2019

Revised: November 7, 2019

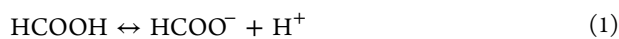
Accepted: November 22, 2019

Published: November 22, 2019

estimate shows that both CO₂ electroreduction products, CO and FA, have a positive business case.^{18–21} However, these initial cost estimates are highly uncertain because (1) there are no commercial-scale CO₂ electrolyzers on the market and (2) downstream separations of dilute (liquid) products are often excluded in the economic analysis. The cost of separating dilute liquid products like carboxylic acids from electrochemical cells should not be underestimated, since the challenges are very similar to those encountered in fermentation processes.^{22–24}

- Complex mixtures. The solution often contains electrolytes, nutrients, and several byproducts.
- Dilute products. The concentration of products is low to prevent microbiological inhibition in fermentation processes and loss through membranes in electrochemical cells. Similarly, current product concentrations from the CRR are mostly in the mmol range.
- Relatively high pH solutions. The microbiological production of carboxylic acids is typically performed at 5.5 < pH < 7.0, while CO₂ electrolyzers are more efficient in alkaline conditions. In both cases, the acid almost completely dissociates into the carboxylate form.
- Complex downstream processing. The recovery of products is one of the key bottlenecks in fermentation processes and can account for >30% of the total processing cost. Similar cost of merits can be expected for the separation of (dilute) products from electrochemical processes.

Recently, De Luna et al.⁴ and Greenblatt et al.²⁵ have highlighted the importance of downstream separation of products from electrochemical cells. The key message is that even with an FE of 100% and high current densities, the economic viability of the CO₂ electroreduction process will depend on the success of the downstream separation, especially for liquid products. The separation of small carboxylic acids from aqueous solutions is by no means trivial. In fact, the separation of formic acid or acetic acid from water falls under one of the most challenging systems in the chemical industry. These molecules show a complex self-association (dimer and chain formation) and strong cross-association behavior with water, including azeotrope formation.²⁶ One of the main reasons for the failure of fermentation processes to penetrate the chemical industry is related to the difficulties involved in product recovery.²² The electrochemical reduction of CO₂ in aqueous media is typically performed at alkaline conditions to suppress the competing hydrogen evolution reaction (HER). As a consequence, formic acid, which has a pK_a of 3.75, will almost completely dissociate into the formate form according to the reaction



The degree of dissociation depends on the pH and can be computed from the Henderson–Hasselbalch equation. Of course, it is possible that in a solution the proton is exchanged with the cation of the alkaline electrolyte (salt). For example, using potassium bicarbonate (KHCO₃) as the catholyte will yield potassium formate (HCOOK), which essentially means that the electrolyte is consumed in the process. Furthermore, the protonation of formate to formic acid in acidic media does not necessarily need to occur on the electrode surface; it can equally well happen in the solution with protons from a cation-exchange membrane (CEM) or a bipolar membrane (BPM). Although electrochemists do not distinguish between both forms—formic acid and formate are interchangeably used in the literature—it

has major implications for the downstream separation. As will be shown later, the selection of a proper downstream process depends on the dissociation state of the acids.

In this work, a high-pressure semicontinuous batch electrolyzer with a Sn-based cathode is used to convert CO₂ to formic acid in low-pH aqueous electrolyte solutions. The effect of CO₂ pressure (between 10 and 50 bar), electrolyte (K₂SO₄) concentration, and bipolar membranes (BPMs) on the Faraday efficiency and current density was investigated. A bipolar membrane consists of two layers, a cation-exchange layer and an anion-exchange layer, which are laminated together.^{27–30} Between the two layers, an interfacial region is formed where water splitting occurs upon application of a sufficiently high voltage. The protons are then used in the CRR or in the HER at the cathode, while the hydroxide ion is discharged at the anode. Recently, we have used BPMs in a high-pressure electrolyzer to convert CO₂ to formate.³¹ Bipolar membranes for CO₂ electrolysis have some advantages over monopolar membranes, since BPMs (1) show a lower product crossover, (2) maintain a constant pH-gradient over the membrane, (3) can prevent carbonate/bicarbonate formation in gas diffusion electrode (GDE)-based CO₂ electrolyzers, and allow for the integration of CO₂ capture and conversion.^{31–38} Here, for the first time, a BPM is used to convert high-pressure CO₂ to formic acid. Note that an aqueous solution of K₂SO₄ has a neutral pH, but it becomes acidic upon dissolution of high-pressure CO₂. To the best of our knowledge, only Mahmood et al.³⁹ and Scialdone et al.⁴⁰ have reported (efficient) CO₂ electrolysis in acidic media to FA. Many others have focused on CO₂ electrolysis to formate or wrongly claimed to produce FA while operating at alkaline conditions. We will show that the subtle difference between the dissociated (ionic) and the undissociated (neutral) acid has major consequences for the selection of the downstream process. By applying common separation heuristics, liquid–liquid extraction and electrodialysis (ED) were selected for the separation of formic acid and formate, respectively. An economic analysis for both separation methods has been performed, which shows that formic acid should be preferred over formate as a product of the CO₂ electrolysis process.

■ EXPERIMENTAL SECTION

The details of the high-pressure semicontinuous batch electrolyzer can be found in our previous work. Here, only a brief description of the experimental setup will be provided. The high-pressure electrochemical cell, which can be operated up to 80 bar, was divided into two compartments using a bipolar membrane (~160 μm, Fumatech). The volume of the cathodic compartment (~100 mL) was approximately half the volume of the anodic compartment. A tin-based (99.9% Sn, ElectroCell) cathode with a reactive surface area of 80 cm² and an iridium mixed metal oxide (Ir-MMO, MAGNETO Special Anodes) anode with a surface area of 140 cm² were used. All experiments were performed at room temperature (22 ± 1 °C). The pressure of the cell was measured with a manometer (Swagelok) with an accuracy of ±1 bar. The electrolytes potassium hydroxide (99.5%) and potassium sulfate (K₂SO₄) were purchased from Sigma-Aldrich. A 1 M KOH solution and three different concentrations of K₂SO₄ (0.125, 0.25, and 0.5 M) were used as the anolyte and catholyte, respectively. The catholyte was pressurized with high-pressure CO₂ (99.99%, Linde Gas) from a gas cylinder and recirculated for one hour with a high-performance liquid chromatography (HPLC) pump (10 mL/min, Varian ProStar 210) until saturation. Subsequently, the

electrochemical experiments were performed for 20 min at a fixed cell potential using a benchtop lab power supply (Voltcraft DPPS-16-40). Both compartments were emptied after the end of each experiment, and the catholyte was analyzed for formic acid using an ion-chromatograph (Dionex DX-120, 4 mm AG14/AS14 guard and analytical column). A pure standard of formic acid was purchased from Sigma-Aldrich to calibrate the equipment for quantitative analysis. A mixture of 1 mM Na₂CO₃ and 1 mM NaHCO₃ solution with a flow rate of 1 mL/min was used as the eluent. Note that an ion-chromatograph cannot distinguish between the dissociated or undissociated form of FA, but the concentration is obtained as the sum of both species because the alkaline eluent converts the (neutral) acid molecules to the ionic form. Nevertheless, once the pH of the sample is known, the Henderson–Hasselbalch equation can be used to calculate the speciation. The pH of the samples from the reactor was measured with a Metrohm 914 pH/conductometer. The gaseous products were not analyzed because taking a well-mixed gas sample in our high-pressure batch electrolyzer is not straightforward. The reason for this is that the cathode compartment is in direct contact with a high-pressure CO₂ buffer vessel, which is purged regularly to prevent accumulation of byproducts. For this reason, it is not possible to obtain a homogeneously mixed gas sample from the high-pressure vessel. However, test results from our continuous scale electrolyzer, which will be published in the near future, show that the majority of the gaseous byproducts (>99%) is hydrogen. The bipolar membranes were susceptible to blistering, which was likely caused by an abrupt shutdown of the power supply and pressure changes. Therefore, a new membrane was used after 15 pressurizing/depressurizing cycles of the reactor. The electrochemical experiments were repeated twice to check the reproducibility of the measurements.

The FE and the CD are two important performance metrics for an electrochemical process. The FE measures the selectivity of charge transfer in an electrochemical reaction to the desired product, while the CD is equivalent to the reaction rate. The FE (%) for formic acid/formate is calculated from

$$FE = \frac{FnVC^{\text{exp}}}{ItM_w} \times 100\% \quad (2)$$

where I is the output current (A = C/s), t is the total time of the measurements (s), M_w is the molecular weight of formic acid (g/mol), n is the number of electrons transferred in the reaction (2 for formic acid/formate), V is the volume of the catholyte (m³), C^{exp} is the experimentally measured concentration of formic acid/formate (g/m³), and F is the Faraday constant (C/mol). By neglecting the covariance, an estimate of the uncertainty in the FE can be obtained from the individual uncertainties of the variables in eq 2 using the methods of error propagation⁴¹

$$\frac{\delta FE}{FE} = \sqrt{\left(\frac{\delta V}{V}\right)^2 + \left(\frac{\delta C}{C}\right)^2 + \left(\frac{\delta I}{I}\right)^2 + \left(\frac{\delta t}{t}\right)^2} \quad (3)$$

The estimated uncertainties in V (± 1 mL due to purging/depressurizing), C ($\pm 1\%$ due to the accumulated accuracy of the analytical equipment), I (± 0.05 A due to the accuracy of reading the power supply), and t (± 20 s due to manual start/shutdown of the power supply) result in an uncertainty of ca. 5% in FE.

The CD is obtained by taking the ratio of the output current and the geometrical surface area of the cathode (~ 80 cm²) exposed to the solution. The output current fluctuated during

the experiments; therefore, the total charge passage (Q) was obtained by integrating the current versus time ($I-t$) curve

$$Q = \int_0^t I dt \quad (4)$$

The accuracy of the lab power supply was ± 0.05 A, which renders an uncertainty of approximately 60 C on Q for an experiment of 20 min or an uncertainty in the current density of ~ 0.6 mA/cm². The error due to the numerical integration of the ($I-t$) curve is within this uncertainty.

RESULTS AND DISCUSSION

In the following, the effects of CO₂ pressure, electrolyte concentration, and cell potential on the CRR to FA are discussed. Subsequently, the challenges related to the downstream separation of formic acid and formate from electrochemical cells are outlined. Finally, the economic viability of the formic acid or formate process, including downstream separation costs, is assessed.

Effect of Pressure. The electrochemical experiments were performed at 3.5 V for CO₂ pressures between 10 and 50 bar. The used anolyte, catholyte, and flow rate were 1 M KOH, 0.25 M K₂SO₄, and 10 mL/min, respectively. The results are shown in Figure 1. The FE, CD, and concentration of FA are

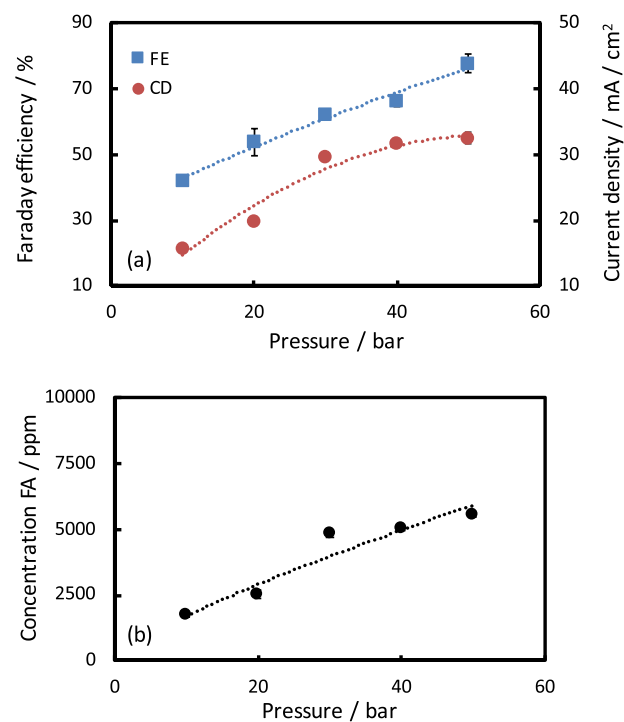


Figure 1. Effect of pressure on the (a) FE and (b) CD at a cell potential of 3.5 V using a bipolar membrane with 1 M KOH as the anolyte, 0.25 M K₂SO₄ as the catholyte, and a flow rate of 10 mL/min. The lines are polynomial fits to guide the eye.

significantly increased by elevating the pressure. The FE increases steadily from 40% at 10 bar to 80% at 50 bar, but the pressure effect is expected to flatten out at higher pressures. This is due to the fact that the solubility of CO₂ in water at room temperature does not increase considerably beyond a pressure of 50 bar and some FA is transported through the bipolar membrane to the anode compartment. The anolyte was analyzed to estimate the crossover of FA, which increased

with pressure and CD. Approximately 2–4% of the produced FA was found in the anode compartment, where the higher value corresponds to the highest pressure and CD. In our previous study, the crossover of formate through bipolar membranes was found to be $\sim 1\%$. Therefore, the crossover rate of formic acid is higher than that of formate, which is better retained by the charged layers of the membrane. Overall, an FE of 80% is attainable at a CD of 30 mA/cm^2 , which results in an FA concentration of around 0.6 wt %. Recently, we have studied CO_2 electrolysis in KHCO_3 solutions, which resulted in a maximum FE of around 90% for formate at similar conditions. The slightly lower FE in K_2SO_4 solutions is due to the acidic reaction environment caused by high-pressure CO_2 dissolution, which favors the HER. At the end of the experiments, the pH of all catholyte samples was between 2 and 3, which confirms that more than 90% of the formic acid was in the undissociated (molecular) form. Increasing the pressure is thus an interesting option to improve the efficiency of CO_2 electroreduction even in a slightly acidic medium. In Figure 2, the effect of pressure on the

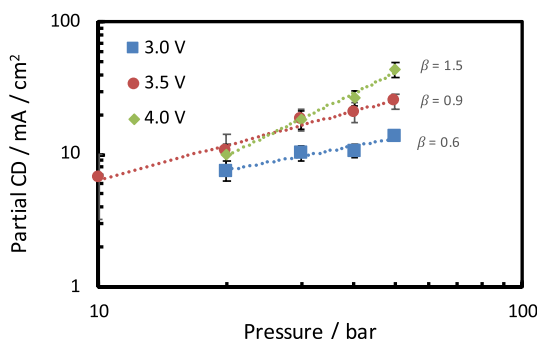


Figure 2. Effect of pressure on the rate of CO_2 electroreduction at 3.0 V (squares), 3.5 V (circles), and 4.0 V (diamonds). The lines represent the equation $i_{\text{CO}_2} = kP_{\text{CO}_2}^\beta$, where i_{CO_2} is the partial current density of CO_2 , k is a constant, P_{CO_2} is the partial pressure of CO_2 , and β is the order of the reaction.

rate of CO_2 electroreduction (i.e., the partial current density of CO_2) is shown. The reaction rate is proportional to a fractional power of the CO_2 pressure

$$i_{\text{CO}_2} = kP_{\text{CO}_2}^\beta \quad (5)$$

where i_{CO_2} is the partial current density of CO_2 , k is a constant, P_{CO_2} is the pressure of CO_2 , and β is the reaction order. By plotting $\log(i)$ vs $\log(P)$, the values of β obtained at 3.0, 3.5, and 4.0 V are 0.6, 0.9, and 1.5, respectively. We note that at 4.0 V, the HER is dominating the CRR, which is severely limited by mass transfer. Therefore, the order of the reaction obtained at 4.0 V might be questionable. However, Vassiliev et al.,⁴² Eyring et al.,^{43,44} and Proietto et al.⁴⁵ also observed a potential dependent order of the reaction. Vassiliev et al.⁴² obtained similar values of β for CO_2 reduction on tin electrodes at pressures up to 25 bars. According to these authors, the fractional reaction order is due to the strong repulsion of adsorbed reacting particles, which participate in the rate-determining step of the reaction. Furthermore, the dependence of the reaction rate on the CO_2 pressure (or concentration) indicates that a high degree of surface coverage is not achieved even at a pressure of 50 bar.

Effect of Electrolyte Concentration. It is well-known that the type and concentration of the electrolyte can have an impact on the electroreduction of CO_2 . Therefore, three different

concentrations of K_2SO_4 (0.125, 0.25, and 0.5 M) were used as the catholyte. The cell potential, anolyte, and the flow rate were 3.0 V, 1 M KOH, and 10 mL/min, respectively. The effect of the electrolyte concentration on the FE and CD is shown in Figure 3. The best results in terms of the FE are obtained for moderate

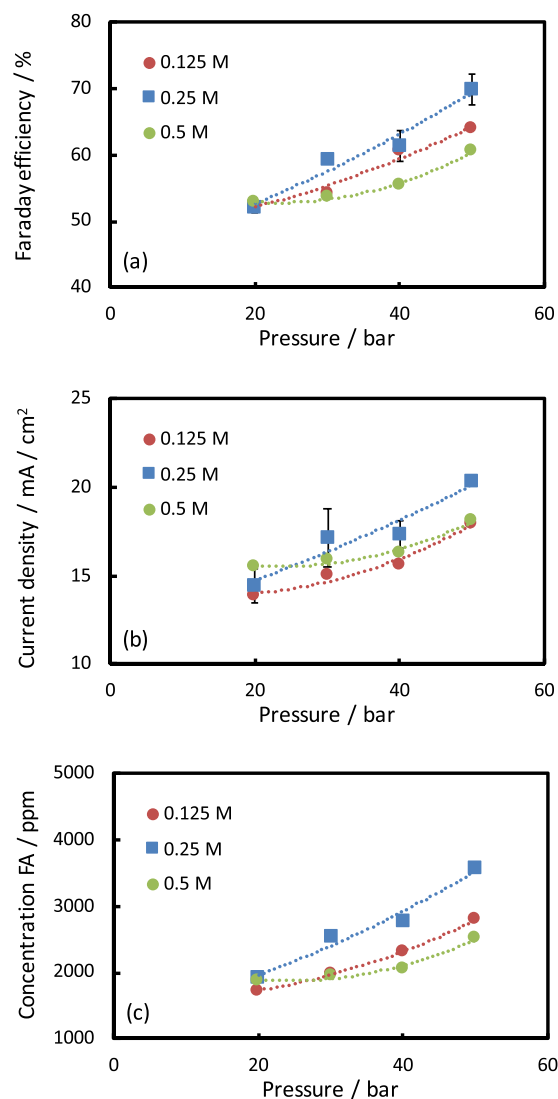


Figure 3. Effect of catholyte concentration (0.125, 0.25, and 0.5 M K_2SO_4) on the (a) FE, (b) CD, and (c) FA production as a function of pressure at 3.0 V using a bipolar membrane with 1 M KOH as the anolyte and a flow rate of 10 mL/min. The lines are polynomial fits to guide the eye.

(0.25 M K_2SO_4) electrolyte concentrations. Furthermore, using a high electrolyte concentration (0.5 M K_2SO_4) has a dramatic effect on the performance of CO_2 electrolysis because the salting-out effect significantly reduces the CO_2 solubility. On the other hand, using a low electrolyte concentration (0.125 M) causes conductivity problems and the pH drop due to CO_2 dissolution is higher, which favors the HER. These results are in agreement with Li and Oloman,⁴⁶ Zhong et al.,⁴⁷ and Ramdin et al.,³¹ where a moderate KHCO_3 concentration was found to work the best.

Effect of Cell Potential. The applied potential has a huge impact on the product distribution in a CO_2 electrolyzer. Therefore, the effect of cell potential on the FE and the CD was

investigated. In addition to the experiments at 3.5 V, CO₂ electrolyses were also performed at 3.0 and 4.0 V in 0.25 M K₂SO₄ solutions. In all of these experiments, the anolyte and flow rate were fixed at 1 M KOH and 10 mL/min. The results for the different cell potentials are shown in Figure 4. The FE, CD,

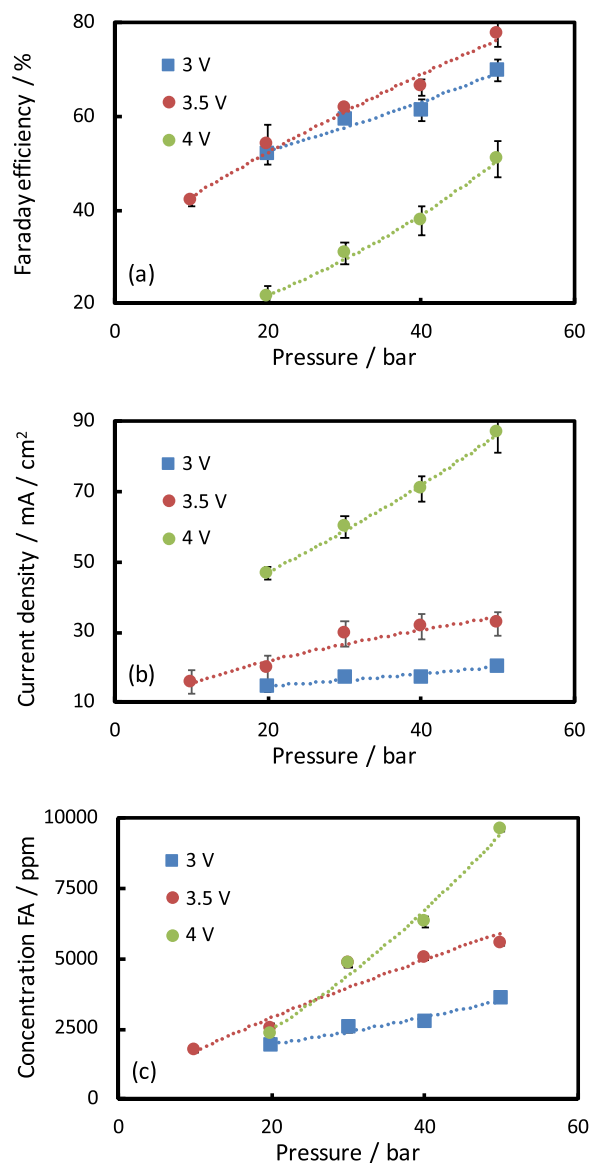


Figure 4. Effect of cell potential (3.0, 3.5, and 4.0 V) on the (a) FE, (b) CD, and (c) FA production as a function of pressure using a bipolar membrane with 1 M KOH as the anolyte, 0.25 M K₂SO₄ as the catholyte, and a flow rate of 10 mL/min. The lines are polynomial fits to guide the eye.

and FA concentrations increase with pressure for all potentials. The highest FE is obtained at 3.5 V with a corresponding CD of 30 mA/cm². The CD increases significantly at 4 V, but the FE for FA drops dramatically, which means that the formation of byproducts (e.g., hydrogen) is promoted. Hydrogen production is dominant at 4 V due to a combined effect of enhanced water splitting of the BPM and an increased water reduction at the cathode. At high potentials, the CO₂ at the electrode is depleted quickly and mass transfer starts to limit the process even at high pressures. On the other hand, at low potentials (e.g., 3 V) the process is kinetically limited, which also affects the FE.³¹ In

summary, it remains a challenge to simultaneously obtain a high FE and CD. Given this trade-off, different properties can be optimized to set the operating conditions for the CO₂ electrolyzer. For example, one can optimize for the FE or CD, the type and concentration of product, the energetic efficiency, and/or the power input. In practice, the optimization decision is based on the overall process economics, which depends on many factors like the price of electricity and feedstocks, market value of products, lifetime of reactor components, and downstream processing costs.

State-of-the-Art of CO₂ Electrolysis to Formic Acid/Formate. In the following, we will briefly discuss the latest efforts and achievements concerning the electrochemical conversion of CO₂ to FA/formate. In Table 1, an overview of the current status of CO₂ electrolysis to formic acid/formate is provided. These data can be used as a benchmark for future studies and to set realistic values for (downstream) process design variables (e.g., FE, CD, product concentrations, impurities, power input, etc.). For any electrochemical process, it is desired to have as high as possible FE, CD, or production rate and product concentration at a minimum power input, which is related to the cell potential. Initial techno-economic studies of CO₂ electrolysis to chemicals/fuels indicate that a CD of >100 mA/cm² at a cell potential of <3 V with an FE of >90% is required to compete with commercial processes.^{4,8,18–21,48}

However, a comparison of the data in Table 1 shows that this remains an elusive goal for CO₂ electrolysis to FA. Recently, considerable progress has been made to resolve some of the problems associated with the electrochemical reduction of CO₂ in the liquid phase. As shown by Alvarez-Guerra et al.,⁴⁹ the poor solubility of CO₂ in aqueous electrolyte solutions at ambient conditions causes significant mass transfer limitations, which leads to a low FE and/or CD. More importantly, it results in a very dilute product stream, which is mainly a consequence of using excess water. As shown by Proietto et al.⁵⁰ and Ramdin et al.,³¹ the CO₂ solubility and the performance of the electrochemical reactor in terms of the FE and CD can be improved by elevating the pressure. The product concentration was increased by recycling the catholyte, which can result in product losses due to the transport of FA through the membrane and subsequent oxidation at the anode. Furthermore, relatively high (>3.5 V) cell potentials (i.e., power input) were required to obtain high current densities. Gas diffusion electrodes (GDEs) have been proposed to overcome some of the limitations imposed by the liquid-phase reduction of CO₂. As shown by Kopljar et al.,⁵¹ Del Castillo et al.,⁵² Irtem et al.,⁵³ and Yang et al.,⁵⁴ the use of GDEs can yield significant improvements in terms of the power input (i.e., lower cell voltage), CD, and production rate. Moreover, the concentration of FA/formate is higher for GDE-based CO₂ electrolysis, since it is no longer required to dissolve CO₂ in excess water. A relatively new development in the field of CO₂ electrolysis is the use of catalyst-coated membranes (CCMs).⁵⁵ Díaz-Sainz et al.⁵⁶ have used a CCM to convert humidified CO₂ to formate with an FE of around 50% at a CD of 45 mA/cm² but at a cell potential of only 2.25 V. The study of Lee et al.⁵⁷ is interesting in many ways, since a CCM-GDE was used to convert humidified CO₂ to concentrated formate (4 wt %) with a very high FE (>90%) and a CD of 50 mA/cm² at just 2.2 V. Depending on the vapor supply rate, an even higher concentration of formate (11.6 wt %) could be obtained, but at an expense of a lower FE (77.7%). Recently, Xia et al.³⁸ reported the use of solid electrolytes and two-dimensional bismuth (2D-Bi) electrodes for CO₂ reduction to formic acid in

Table 1. Comparison of CO₂ Electrolysis to Formic Acid/Formate in Continuous-Flow Electrolyzers Using Sn- or Bi-Based Gas Diffusion Electrodes (GDE), Plates, and Catalyst-Coated-Membrane (Gas Diffusion) Electrodes (CCM-GDE)

conditions	ref 51	ref 52	ref 54	ref 49	ref 50	ref 53	ref 57	ref 56	ref 38	this work
product	formate	formate	FA	formate	FA	formate	formate	formate	FA	FA (formate) ^d
mode of operation	single pass	single pass	single pass	single pass	recycled	recycled	single pass	single pass	single pass	recycled
temperature (K)	ambient	ambient	ambient	ambient	ambient	ambient	343	293	298	295
pressure (bar)	1	1	1	1	30	1	1	1	ambient	50
cathode	SnO ₂ /C-GDE	Sn/C-GDE	Sn/C-GDE	Sn plate	Sn plate	Sn-GDE	Sn/CCM-GDE	Sn-CCM	2D-Bi GDE	Sn plate
anode	Pt/C CCM	Ir-MMO	IrO ₂	Ir-MMO	Ti/IrO ₂ -Ta ₂ O ₅	DSA/O ₂	Pt black	Ir-MMO	IrO ₂ -C	Ir-MMO
anode reaction	HOR	OER	OER	OER	OER	OER	OER	OER	OER	OER
cation-exchange membrane	Nafion 117	Nafion 117	Nafion 324	Nafion 117	no membrane	Nafion 117	Nafion 115	Nafion 117	Nafion 117	BPM
anion-exchange membrane (AEM)			Sustainion		no membrane				Sustainion	BPM
surface area of cathode (cm ²)	2.7	10	5	10	9	10.2	25	10	4	80
catholyte flow [mL/(min cm ²)]	0.37	0.07	0.02 (0.001) ^c	2.3	3.3	2	0.002 ^b	0.001 ^b	0.07 (0.001) ^c	0.125
cell voltage (V)	2.5	4.3	3.3	2.79	6.5 ^a	2.8	2.2	2.25	3 (3.25)	3.5
current density (mA/cm ²)	1.33	200	140	12.25	50	10	55.4	45	30 (100)	30 (35)
concentration of FA (wt %)	0.46 ^a	1.68	9.4	0.005	1.26	0.08	4.15	1.92	0.51 (29)	0.6 (1)
Faraday efficiency of FA (%)	81	42.3	94	71.4	82.5	71	93.3	49.4	80 (30)	80 (90)
production rate [mmol/(m ² s)]	5.58	4.38	6.8	0.46	2.1	0.4	2.7	1.15	1.24	1.2 (1.6)
max. operation time (h)	3	1.5	142	1.5	60	6.00	48	1.5	100	0.33

^aData obtained from Kopjar et al.⁵¹ and Proietto et al.⁵⁰ through personal communication. ^bSupply of water vapor to the cathode. ^cData in brackets are for the low flow rate of deionized water in the center compartment. Note that the flow rate was normalized with the electrode area for consistency reasons but is not strictly necessary for flow in the center compartment. ^dData in brackets are from our previous work³¹ for CO₂ electrolysis in alkaline media to formate.

a three-compartment cell. The center compartment was filled with a proton conducting or a formate conducting solid electrolyte. Depending on the type (i.e., deionized water or nitrogen) and flow rate of the purging fluid, Xia et al.³⁸ obtained a very concentrated formic acid solution in the center compartment. Using a deionized water flow rate of 0.3 mL/h, a formic acid concentration of around 29 wt % could be obtained at 100 mA/cm² but with an FE of 30% at a cell potential of 3.25 V. Using humidified nitrogen with a flow rate of 10 sccm to purge the center compartment, a formic acid concentration of 49.3 wt % was obtained at 200 mA/cm² but at an FE of ~40% at a cell potential of 2.75 V. Xia et al.³⁸ demonstrated long-term stability (up to 100 h) of the solid-electrolyte-based process but only at 30 mA/cm². So far, Yang et al.⁵⁴ reported stable formic acid production for >140 h of operation, achieving an FA concentration of ~10 wt % in a three-compartment cell at 3.5 V with an FE of 94% and CD of 140 mA/cm². Up to 18 wt % FA could be produced in a single pass, but product crossover through the cation-exchange membrane reduced the FE to 30%. In Table 1, a distinction is made between formate and formic acid as a product. To the best of our knowledge, only Mahmood et al.,³⁹ Proietto et al.,⁵⁰ and this work have reported efficient CO₂ electrolysis in acidic media to formic acid. The three-compartment reactor of Yang et al.⁵⁴ and Xia et al.³⁸ also produced formic acid, but this was achieved indirectly by protonating formate in the center compartment. An advantage of the three-compartment process of Yang et al.⁵⁴ and the solid electrolyte cell of Xia et al.³⁸ is that the FA stream does not contain additional electrolytes, which will simplify downstream processing. The center compartment of the process of Yang et al.⁵⁴ and Xia et al.³⁸ was, respectively, filled with ion-exchange resins (IERS) and solid electrolytes to compensate for the low conductivity of FA solutions. Other studies have either concentrated on CO₂ reduction to formate or incorrectly claimed to have produced formic acid while operating at alkaline conditions. The often-overlooked difference between formic acid and formate has major consequences for the selection of the downstream separation process, which is dictated by the dissociation state of the acid (i.e., molecular or ionic form).

It is clear from the foregoing discussion that the liquid-phase CO₂ reduction process has some inherent limitations, even at high pressures, such as the requirement of a relatively high cell potential for a reasonable CD and low product concentrations. Therefore, the design variables (e.g., cell potential, CD, FE, and concentration) for the downstream processing and the economic analysis are based on a CO₂ electrolyzer with gas diffusion electrodes.

Downstream Separation of Formic Acid/Formate. In the following, we will assess the suitability of some commonly used downstream processes in the chemical industry for FA/formate separation from electrochemical cells. From Table S2 it becomes apparent that FA has a very similar boiling point as water and a mixture of both exhibits an azeotrope. It is informative to investigate the phase behavior of FA–water mixtures. In Figure 5, the *T*_{xy}-diagram of water and FA mixtures for different pressures is shown. This system forms a high boiling azeotrope, which means that the azeotropic mixture containing 77.6 wt % FA at atmospheric pressure has a higher boiling point than the pure constituents. The concentration of FA in the azeotropic mixture, see the solid line in Figure 5, can be increased by elevating the pressure, but this will also raise the boiling point of the mixture, which is not desired as FA is susceptible to decomposition at higher temperatures. Note that

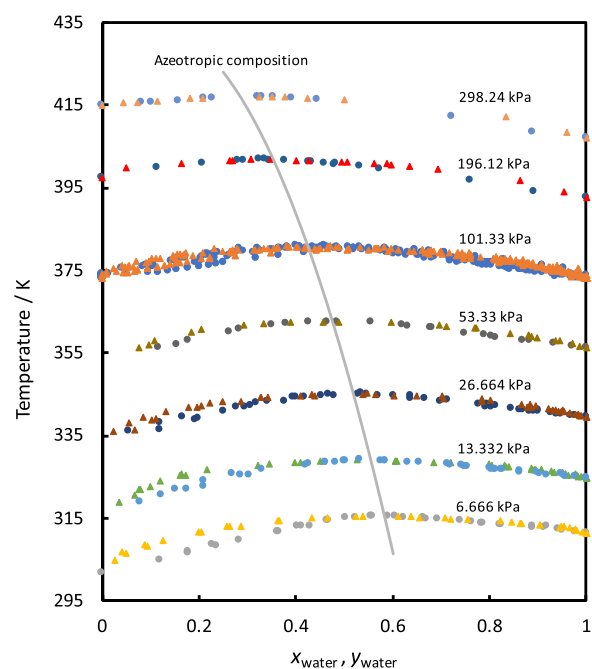


Figure 5. Vapor–liquid equilibrium (VLE) data of the system water–formic acid at different temperatures and pressures. Bubble points, dew points, and azeotropic compositions are denoted by circles, triangles, and solid lines, respectively. Experimental data taken from Gmehling et al.⁵⁸

the azeotrope disappears at high pressures (>40 bar), but in practice, FA distillation is not performed in excess of 3–4 bar due to the aforementioned problems. Nevertheless, a combination of distillation under pressure followed by vacuum distillation can be used to obtain high-purity FA. Figure 5 also shows that close to or higher than the atmospheric pressure, formic acid is the high boiling component and will leave the column as bottoms. Interestingly, at vacuum conditions, formic acid is the more volatile component and will leave the column as distillate. This observation is relevant for preventing solid formation in the column due to crystallization of electrolytes/salts upon water removal. The investment and operating costs of a formic acid plant depend strongly on the desired concentration, which is reflected in the price of different grades of formic acid on the market. BASF supplies globally five different grades of FA (i.e., 85, 90, 94, 95, and 99 wt %), but in Europe/Asia only 85, 94, and 99 wt % are available. Other companies like Eastman and Perstorp also supply 75 wt % of FA solutions. Here, the downstream process will be designed to deliver at least 85 wt % of FA.

Distillation, due to its simplicity and scalability, is often preferred over other methods to separate volatile components. However, ordinary distillation is not suitable when azeotropic or isomeric mixtures are involved, the solute concentration is too low, the materials are heat sensitive, separation of strong hydrogen-bonding molecules from water is required, and the solute is nonvolatile (e.g., formate). Distillation is impractical for the separation of FA from (photo)electrochemical cells because typical concentrations are less than 10%, which would require removal of large amounts of water.

Extraction has traditionally been used to separate dilute carboxylic acids (<30 wt %) from aqueous streams (e.g., fermentation broths).^{59,60} The main difference with distillation is that the components are not separated based on their boiling

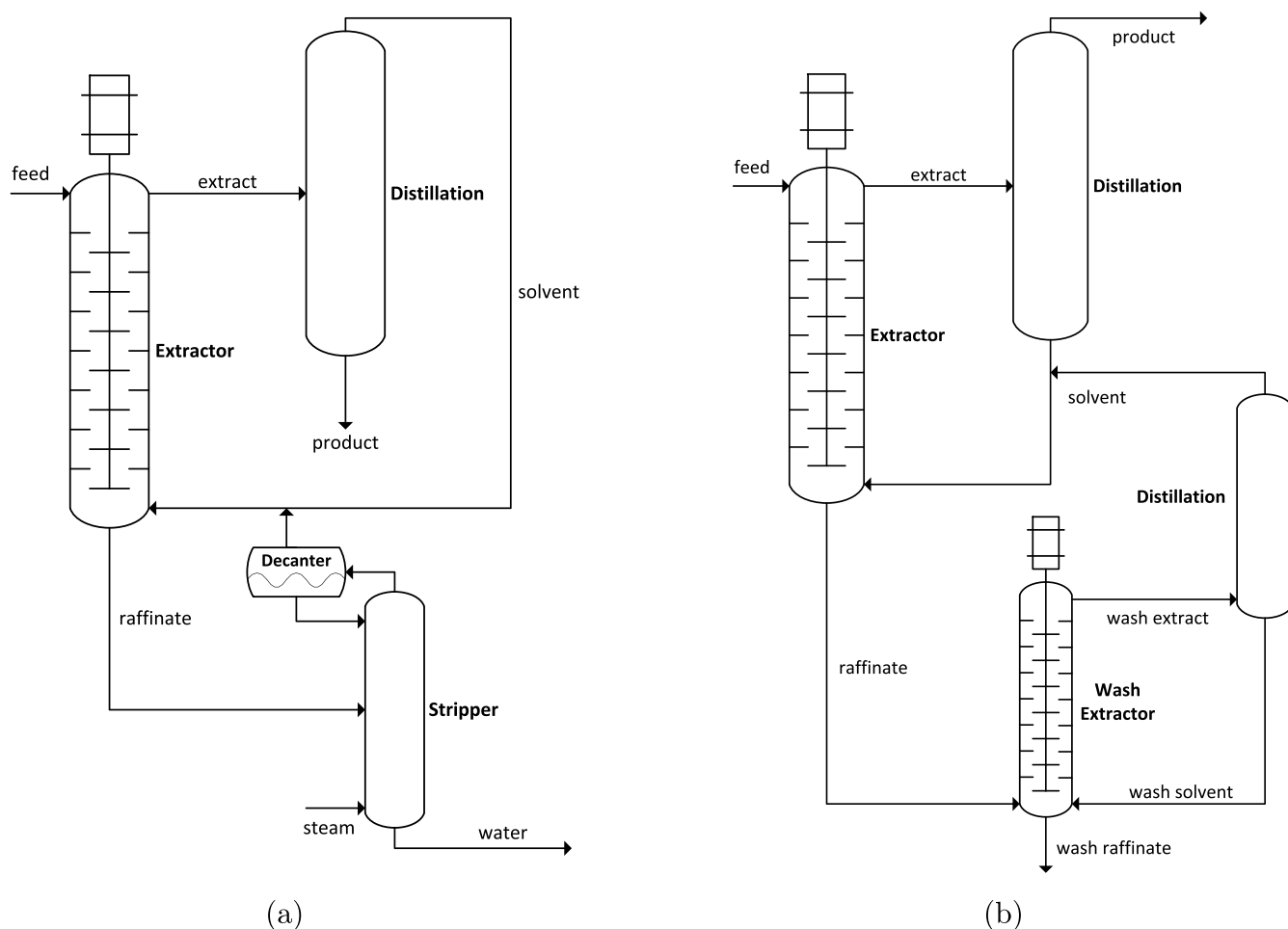


Figure 6. Simplified extraction process to recover dilute products. (a) A low boiling solvent is used to extract a product from dilute streams. The extract containing the solvent and the product is introduced into the distillation column, where the solvent is recovered as tops and recycled back to the extractor, while the product leaves the column as bottoms. For water-soluble solvents, raffinate treatment is required to prevent loss of extractants and to meet environmental regulations. Typically, steam is used to strip out the solvent, which can be recycled to the extraction unit. Water from the stripper can be recycled to the process. (b) A high boiling solvent is used to extract the product. The process is similar to the low boiling solvent case, except that the bottoms and tops in the product distillation column are reversed and a more complicated raffinate treatment is required. A wash extractor is used to back-extract the high boiling solvent, which is regenerated in a second distillation column. Depending on the boiling point of the wash solvent, the bottoms and tops of the second distillation column might be reversed.

points but rather on their affinity to bind the extraction solvent. For liquid–liquid extraction, the solute is transferred from one liquid phase (i.e., the feed/carrier solvent) to the second liquid phase (i.e., the extraction solvent).^{61,62} Note that extraction is never a stand-alone process, since it requires at least one additional step (e.g., distillation) for solvent recovery, but it may also include one or more product purification steps. Therefore, the capital cost of an extraction process is often higher than that of distillation. In the cases mentioned above, the operational costs for distillation to remove large amounts of water may far outweigh the capital costs for liquid–liquid extraction. In Figure 6, a simplified diagram of an extraction process using (a) a low boiling solvent and a (b) high boiling solvent is shown.^{63–66} Comparing the two process configurations shows that the raffinate treatment for high boiling solvents is more complicated and capital intensive. For an efficient separation, the extraction solvent should ideally have the following properties.^{59,61,62,67–71}

- High affinity for the solute: the solute should have a high solubility in the solvent to minimize the number of stages and solvent flows.

- Low miscibility with the feed/carrier solvent: the amount of solvent in the raffinate, which is governed by the miscibility, needs to be minimized to avoid expensive recovery steps.
- Density difference with respect to the feed/carrier solvent of greater than 5%: the two liquids in an extraction column are separated by settling, which is driven by the density difference between both solvents.
- High thermal/chemical stability: the solvent should not degrade/react upon contacting and regeneration.
- High selectivity for the solute: the solvent should only extract the solute and leave other components of the feed unaltered. This corresponds to a high distribution coefficient of the main solute with respect to the other components.
- High boiling point: for ease of material handling, it is desired to have a high boiling solvent, which is completely immiscible with the carrier solvent. However, for high boiling water-miscible solvents, the raffinate treatment step is more complicated.

- Easy regeneration: the solvent in the extract (and raffinate, when the solvents are not completely immiscible) must be separated and recycled back to the extractor. Therefore, solvents that form an azeotrope with the product or have high mutual solubilities should be avoided.
- Low viscosity: it is desired to have a low viscous solvent (<10 cp) to minimize difficulties with pumping, dispersion, and mass transfer.
- Intermediate interfacial tension (5–30 mN/m): the interfacial tension has an impact on the dispersion of droplets. A low interfacial tension will cause emulsification, while a high value will require an increased energy input to create droplets, which also have a higher tendency for re-coalescence.
- Low corrosivity: the extraction solvent should be less corrosive than the feed solution to avoid the use of special construction materials.
- Nontoxic and nonflammable: the solvent should have a low toxicity and flammability to prevent health, safety, and environmental issues.
- Low cost and commercial availability: the solvent should be available commercially at a reasonable price for large-scale applications. Loss of small amounts of highly costly solvents (e.g., through the raffinate) is disastrous for the economics of the extraction process.

In practice, it is difficult to find a solvent that satisfies all of these requirements of an ideal solvent. Often, a screening study is required to select the best solvent for a specific application. For the extraction of carboxylic acids from aqueous solutions, many different types of chemical and physical solvents have been reported in the literature. These solvents can be classified as hydrocarbons, halogen-containing, oxygen-containing, phosphorus-containing, sulfur-containing, nitrogen-containing, and mixtures of the aforementioned compounds. The mechanism of FA extraction in chemical solvents is different from that of physical solvents. In the former, FA is extracted through chemical complexation, while in the latter physical interaction or solvation is the main mechanism of extraction. Efficient extraction of formic acid requires breaking of relatively strong water–FA and FA–FA hydrogen bonds, which is more effectively accomplished by chemical solvents than by physical solvents. Furthermore, chemical solvents typically comprise a mixture of extractants and diluents, which are often difficult to regenerate/recover from the extract and raffinate. The distribution coefficient and the separation factor are two important parameters for screening solvents of extraction processes. The distribution coefficient measures the ability of a solvent to extract the solute from the carrier solvent and is defined as the ratio of the mass concentration of the solute in the organic-rich (extract) phase and the water-rich (raffinate) phase⁶⁷

$$D_{\text{FA}} = \frac{C_{\text{org}}^{\text{FA}}}{C_{\text{H}_2\text{O}}^{\text{FA}}} \quad (6)$$

A high as possible value of D is desired, but it remains challenging to find (chemical or physical) solvents with $D > 10$. In shortcut calculations, often the partition ratio in Bancroft coordinates (K_{B}) is used, which is defined as⁶⁷

$$K_{\text{B}} = \frac{C_{\text{org}}^{\text{FA,wfb}}}{C_{\text{H}_2\text{O}}^{\text{FA,sfb}}} \quad (7)$$

where $C_{\text{org}}^{\text{FA,wfb}}$ and $C_{\text{H}_2\text{O}}^{\text{FA,sfb}}$ are the mass concentrations of FA in the organic phase and aqueous phase on a water-free basis and a solvent-free basis, respectively. An equally important parameter in extraction processes is the selectivity or separation factor of the solvent with respect to other components (e.g., water) in the feed. The separation factor ($S_{i/j}$) is defined as the ratio between the distribution coefficients of the main solute (e.g., FA) and the coextracted component (e.g., water)

$$S_{\text{FA}/\text{H}_2\text{O}} = \frac{D_{\text{FA}}}{D_{\text{H}_2\text{O}}} \quad (8)$$

It is desired to have a high value for S , while $S < 1$ or close to 1 means that separation is not possible. Unfortunately, the separation factors are not always reported in the literature. In Table S1 of the Supporting Information, an extensive compilation of distribution coefficients and separation factors of formic acid in chemical and physical solvents is presented. In Figure 7, the distribution coefficients are plotted as a function of

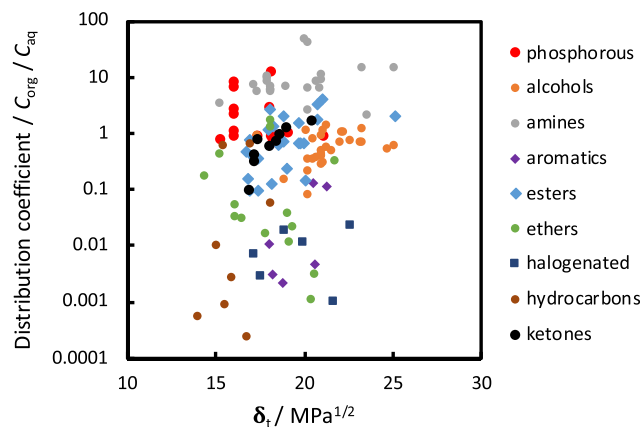


Figure 7. Distribution coefficient of formic acid as a function of the total Hansen solubility parameter of the solvents/diluents at 298.15 K. For the chemical solvents, the solubility parameters of the diluents have been plotted. See the Supporting Information for a compilation of data.^{80–106}

the total Hansen (δ_t) solubility parameter of the solvents or diluents. The correlation of the distribution coefficient with the Hansen solubility parameter is weak, but there are only few extractants with a solubility parameter close to that of formic acid (24.9 MPa^{1/2}). The distribution coefficient of FA in the solvents shows the following trend: amines > phosphorous compounds > esters > ketones \approx alcohols > ethers > aromatics > halogenated compounds > hydrocarbons. Belova et al.⁷² also observed a similar trend of performance. It is clear that chemical solvents (e.g., amines and phosphorous) are superior to physical solvents if distribution coefficients are used as the screening parameter. However, as recently shown by Shah et al.,⁷³ solvent selection should not be based on the partition coefficient only, but solvent cost, product cost, separation factor, thermal stability, and ease of regeneration should be considered as well. An initial screening study was performed to select a number of promising solvents for FA extraction; see Table S3 of the Supporting Information. Note that distribution coefficients and separation factors depend strongly on the FA concentration in

the aqueous phase. The data reported in Table S3 corresponds approximately to an FA concentration of 10 wt % in the aqueous phase. The extractants reported in Table S3 are interesting from the extraction point of view, but the ease of solvent recovery should also be considered in the final selection. In this initial selection, no consideration was given to the possibility of esterification reactions of alcohols and formic acid in the presence of a suitable catalyst (e.g., sulfuric acid). It is unclear to what extent such a reaction will occur in the absence of a catalyst in a distillation column. The mutual solubility of water and the selected solvents is relatively high, which is reflected in the relatively low separation factors reported in Table S3. The consequence of this is that a significant amount of water is coextracted in the organic phase (extract), while the raffinate is polluted with the solvents. For economic and environmental reasons, the solvents need to be recovered from the raffinate. In principle, steam stripping can be used to recover the solvents, since the selected extractants form a low boiling azeotrope with water. Azeotropic data of the solvent–water systems can be found in Table S4 of the Supporting Information. It might seem counterintuitive to recover a solvent with a higher boiling point than water as the distillate, which is only possible for systems that show a low boiling azeotrope at temperatures below the boiling point of water. In all other cases, recovering a high boiling solvent by steam stripping is not practical, since water would be evaporated as a low boiling component, which is a very energy-intensive way of purifying wastewater. In the following, an elimination procedure was used to shortlist the best candidates from Table S3. Avoid solvents that (1) are unstable or react with FA [e.g., *n*-propyl formate and ethyl acetate (hydrolysis)], (2) form a binary and ternary azeotrope with FA and water, which are difficult to separate in a single distillation column (e.g., ethyl acetate and 1-butanol form a ternary azeotrope), (3) have a low selectivity for FA [e.g., diisopropyl ether (DIPE)], (4) are highly miscible with water (e.g., methyl ethyl ketone) and/or have a higher boiling point than FA and forms no or high boiling azeotrope with water or a low boiling azeotrope, which is rich in water content (e.g., 1-hexanol), (5) have a similar density as water [e.g., tributyl phosphate (TBP)], and (6) are not readily available at a low cost (e.g., the high-molecular-weight esters). In a screening study by Veith et al.,⁷⁴ 1-hexanol was found to be a promising solvent for FA extraction. Although 1-hexanol exhibits a relatively high distribution ratio and separation factor, its use has some inherent drawbacks. The 1-hexanol dissolved in water is difficult to recover by steam stripping, since the boiling point of the hexanol–water azeotrope (97.7 °C) is too close to that of water and the water content of the azeotrope is too high (92 mol %). Therefore, 1-hexanol cannot be concentrated and decanted in the stripper but will require an expensive back-extraction process as shown in Figure 6b. Note that diisopropyl ether (DIPE) is sometimes used as an entrainer in azeotropic distillation for formic acid dehydration. DIPE and water form a low boiling azeotropic mixture, which is removed as distillate and condensed in a decanter to form two immiscible liquids. The light organic-rich phase containing DIPE is refluxed to the distillation column, while the water-rich phase containing small amounts of DIPE is sent to the wastewater treatment. Although DIPE is an effective entrainer, it is not suitable for FA extraction from dilute streams due to the low distribution coefficient and separation factor, which is caused by a high solubility of water in DIPE. Similarly, TBP satisfies almost all of the generic requirements of an ideal solvent, except for the relatively high cost and a density that is

very close to that of water. To adjust the density, TBP is often mixed with diluents, which are soluble in water and difficult to recover. For this reason, TBP has been eliminated in the selection. The suitability of butyl acetate and isoamyl alcohol is difficult to judge because no experimental VLE data could be found for the systems butyl acetate–FA and isoamyl alcohol–FA. Methyl isobutyl ketone (MIBK) and FA form a close boiling (not an azeotropic) mixture, which is also difficult to separate as a large number of stages will be required. Finally, 2-methyltetrahydrofuran (2-MTHF) has been selected for FA extraction. Note that 2-MTHF and FA form an azeotrope, which contains 43 wt % 2-MTHF and has a boiling point of 80 °C at 0.5 bar. The 2-MTHF–water azeotrope contains 10.6 wt % water and boils at 71 °C at 1 bar.^{75,76} The FA–water azeotrope contains 22.5 wt % water and boils at 107.7 °C at 1 bar.⁷⁷ Since water is coextracted in the extraction unit, the feed of the distillation column (i.e., the extract) will contain a mixture of FA, 2-MTHF, and water. If the mass ratio of water and 2-MTHF in the feed is slightly higher than the mass ratio of water and 2-MTHF in the 2-MTHF–water azeotrope (10.6/89.4), then it is possible to obtain a concentrated FA stream, essentially free of 2-MTHF, in the bottom of the distillation column. This is in fact an azeotropic distillation process with 2-MTHF as the entrainer. The azeotropic mixture of water and 2-MTHF is distilled over the top of this distillation column, while the bottom is a concentrated FA stream, which is free of 2-MTHF. It is crucial to have a correct amount of water in the feed. For an insufficient amount of water in the feed, the FA stream will be contaminated with 2-MTHF. On the other hand, an excess of water in the feed will dilute the FA stream too much, which would require additional columns for higher concentrations. Hangx et al.⁷⁸ reported a similar azeotropic distillation process to separate FA and 2-MTHF mixtures by addition of water. Tirronen et al.⁷⁹ reported a hybrid extraction–distillation process to separate carboxylic acids using 2-MTHF as the solvent. The amount of water in the extract is a function of the acid content, temperature, amount of salt, and solvent-to-feed ratio. Therefore, by carefully selecting the operating conditions of the extractor, the addition of water can be eliminated. An analysis of the experimental liquid–liquid equilibrium (LLE) data of Demesa et al.⁸⁰ for the system 2-MTHF–FA–water shows that the amount of coextracted water is sufficient to obtain a concentrated FA stream in the distillation column. The recovery of 2-MTHF from the raffinate is relatively easy because it forms a low boiling heterogeneous azeotrope with water at 71 °C, which is well below the boiling point of water at atmospheric pressures. Therefore, steam stripping with a decanter-type condenser can be used to recover the solvent from the raffinate. In the decanter, the low boiling solvent–water azeotrope is condensed and separated into two (immiscible) liquids. The light (organic) phase containing the solvent is recycled to the extractor, while the heavier (aqueous) phase is refluxed to the stripper. It is beneficial to operate the decanter at elevated temperatures because the solubility of 2-MTHF in water is reduced from around 14 wt % at 25 °C to 6.6 wt % at 60 °C, while the solubility of water in 2-MTHF is only slightly temperature dependent (4 wt % at 20 °C to 4.6 wt % at 60 °C).⁷⁵

It is important to note that none of the solvents are able to extract the dissociated (ionic) form of the acid. As shown by Galaction et al.,¹⁰⁷ Hong et al.,¹⁰⁸ Abdelkader et al.,¹⁰⁹ Eyal and Canari,¹¹⁰ Seyd et al.,¹¹¹ and Yang et al.,¹¹² the extraction efficiency of chemical and physical solvents deteriorates as the pH is increased, which corresponds to converting the acid into

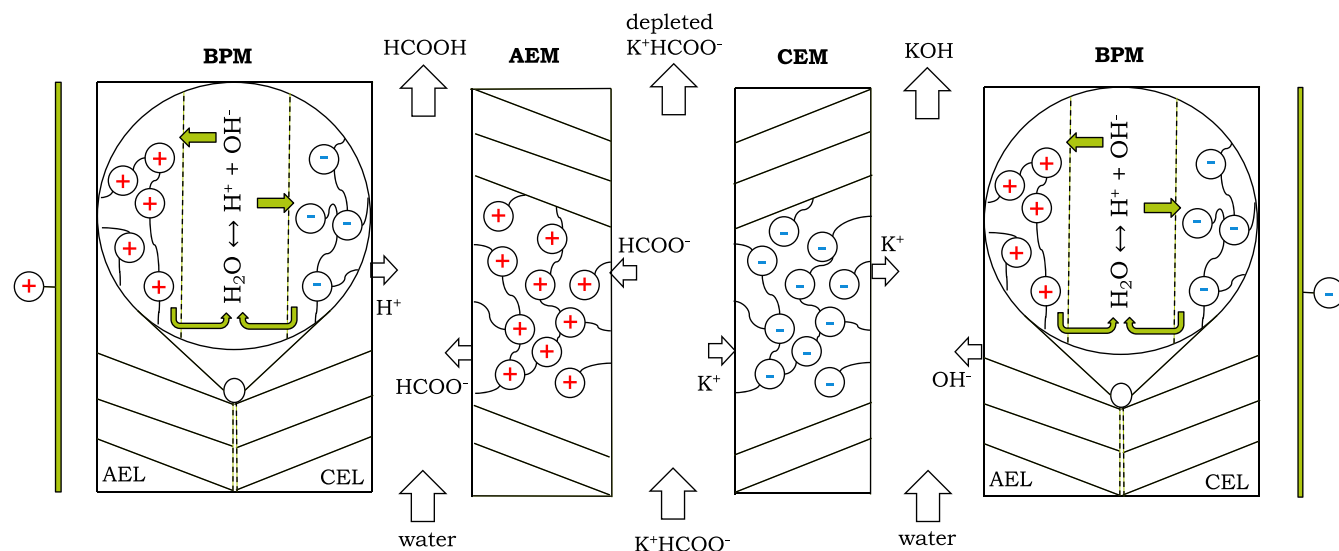


Figure 8. Production of formic acid (FA) from potassium formate solutions using a three-compartment electrodialysis with bipolar membrane (EDBPM) process. A potassium formate solution is fed into the center compartment, which is sandwiched between a cation-exchange membrane (CEM) and an anion-exchange membrane (AEM). The formate ions are pulled through the AEM membrane toward the positive electrode, while the potassium ions migrate through the CEM toward the negative electrode. The formate ions from the AEM and the potassium ions from the CEM combine with the protons and hydroxides from the BPM to produce FA and potassium hydroxide (KOH), respectively. The concentration of FA and KOH can be controlled by the flow of water in the two outermost compartments.

Table 2. Performance of Electrodialysis for Concentrating/Generating FA/Formate Solutions

reactor ^a	configuration ^b	V_{cell} (V)	CD (A/m^2)	FE (%)	P (kWh/kg) ^c	ref
CED	CEM-AEM-CEM	2	55	69	1.4	Nagarale et al. ¹¹⁹
EDBPM	BPM-AEM-CEM	3.6	500	78	2.6	Jaime Ferrer et al. ¹²⁰
EDBPM	BPM-AEM-CEM	3	500	76	2.4	Jamie Ferrer et al. ^{121,122}
EDBPM	BPM-AEM-BPM	5	200	72	4.3	Zhang et al. ¹²³
BEDBPM	BPM-AEM-CEM	1.8	24	87	1.1 ^d	Lu et al. ¹²⁴
CED	CEM-AEM-CEM	8	300	70	3.4	Selvaraj et al. ¹²⁵

^aCED, conventional electrodialysis; EDBPM, electrodialysis with bipolar membranes; BEDBPM, biological electrodialysis with bipolar membranes.

^bMembrane configuration used in the stack, where CEM, AEM, and BPM stand for cation-exchange membrane, anion-exchange membrane, and bipolar membrane, respectively. ^cPower consumption to produce 1 kg of product. ^dIncluding 0.4 kWh/kg bioenergy consumption.

its ionic form. These solvents cannot extract FA/formate from aqueous solutions for $\text{pH} > \text{p}K_{\text{a}}$. Therefore, liquid–liquid extraction is not suitable for separating the formate produced by electrochemical reduction of CO_2 in alkaline media.

Ion-exchange resins (IERS) are also commonly used to adsorb carboxylic acids from fermentation broths. IERS are typically polymeric resins, which are linked with cation- or anion-exchange groups. Strong or weak base resins linked with tertiary or quaternary amines are predominantly used for the separation of carboxylic acids. In Table S5 of the Supporting Information, an overview of literature studies using IERS for FA separation is provided. The basic IERS are efficient in separating FA from a dilute stream, but like in liquid–liquid extraction, only the molecular form of the acid can be removed. As shown by Chanda et al.,¹¹³ Kunin and Myers,¹¹⁴ Husson and King,¹¹⁵ and Lin et al.,¹¹⁶ the adsorption capacity of IERS decreases drastically as the pH is increased, which means that the dissociated form of the acid is not adsorbed. The bottleneck of this process is the regeneration of the resin, which is typically performed by elution with a strong alkaline solution (e.g., NaOH for basic resins). Consequently, a salt product (e.g., NaHCOO) is obtained, which will require acidification to recover the conjugate acid. Acidification can be performed with a strong acid (e.g., H_2SO_4) or an acidic IER, but both methods, the IER upon regeneration,

will produce a waste (e.g., Na_2SO_4) stream. These methods are not consistent with the principles of green chemistry.

Electrodialysis (ED) is an alternative for the unsustainable acid–base reaction process for acidification. In this process, a combination of ion-exchange membranes (e.g., BPM, AEM, and CEM) is used to acidify and concentrate dilute acid and base streams. Luo et al.^{117,118} used electro-electrodialysis and conventional electrodialysis (CED) to concentrate formate solutions. These authors obtained relatively high current efficiencies, exceeding 100% at high FA concentrations due to molecular association, but at relatively low current densities. CED with an AEM and CEM is not so efficient for FA/formate acidification and recovery because of product crossover or leakage through the membranes leading to low current efficiencies. To overcome these issues, electrodialysis with bipolar membranes (EDBPMs) has been proposed. The membranes can be arranged in different configurations to give a two-compartment cell (BPM-AEM or BPM-CEM) or a three-compartment cell (BPM-AEM-CEM). All three configurations suffer to some extent from efficiency loss due to product leakage, which is more pronounced at high current densities and acid or base concentrations. The highest current efficiency is achieved with the three-compartment cell, but at an expense of higher power consumption compared with the two-compartment

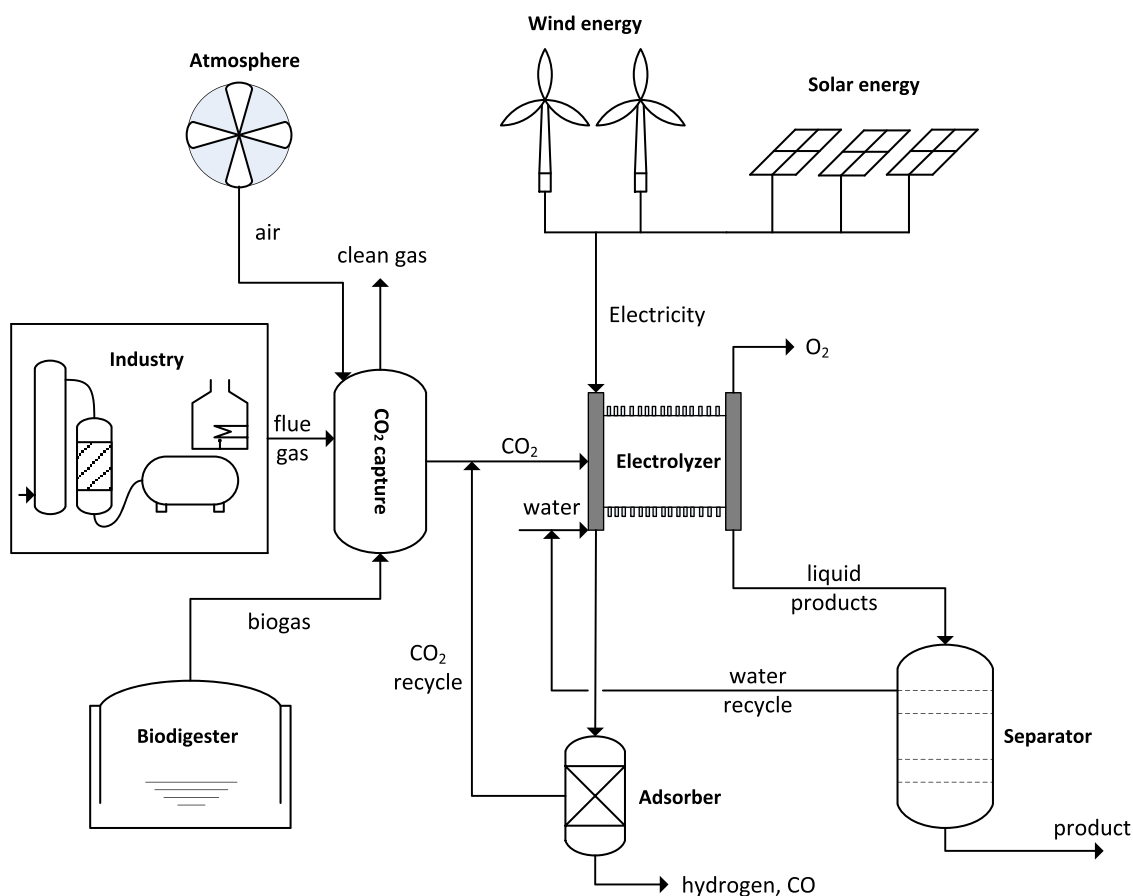


Figure 9. Simplified process diagram of a CO₂ valorization concept including capture, electrochemical conversion, and product separation. An adsorber is used to separate gaseous products and unconverted reactants. The CO₂ capture, recycling/adsorption, and product separation steps may contain additional supporting units, which are not shown.

configurations. In Figure 8, a schematic diagram of a three-compartment EDBPM process for producing formic acid from formate solutions using a BPM-AEM-CEM stack is shown. It is important to note that a dilute formate stream from the electrochemical reactor requires acidification and concentration, while a formic acid stream only requires concentration. Therefore, care must be taken in selecting the membranes, since not all of the three configurations are suitable for concentrating a stream. For example, in the BPM-CEM configuration, the acidification is performed in the feed compartment, which will only protonate the formate, but its concentration will remain roughly the same. In Table 2, an overview of literature studies concerning the conversion and concentration of formate or formic acid solutions using ED is provided. Note that the current efficiency and power consumption reported in Table 2 strongly depend on the current density and initial acid and base concentrations. For moderate current densities, the current efficiency is between 70 and 100% and the power consumption is between 1.5 and 4.5 kWh/kg product. An advantage of the EDBPM process is that it also generates a base, which can be used to capture CO₂ from dilute sources according to the reaction



It is obvious that the integrated CO₂ capture and FA regeneration with EDBPM will improve the economics of the overall process. Conventional processes like distillation or extraction require heat, while electrodialysis runs on power/

electricity, which can be obtained from renewable sources like solar and wind. Therefore, it is more economical to run the electrochemical reactor on excess renewable energy during off-peak hours when the electricity price is low. This strategy is of course applicable to the CO₂ electrolyzer as well.

Crystallization and precipitation are commonly used in the fermentation industry to separate dilute products from broths. In crystallization, the solution is either cooled or evaporated until the solubility limit of the solute is reached or surpassed (supersaturated), causing crystal nucleation. Precipitation is the sedimentation of a sparingly soluble solute from a liquid solution by exceeding its solubility limit. For both processes, the solubility, freezing points, and concentration of the solute are extremely important. These properties of FA solutions and some formate salts are reported in the Supporting Information. It becomes apparent that FA and formate salts are extremely well soluble in water, cause a significant freezing point depression, and have the tendency to undergo supercooling. These all will present a significant challenge to crystallize or precipitate FA out of these solutions. However, the main problem is the low FA/formate concentration (<10 wt %) in the electrochemical cell, which will demand a huge cooling or heating load for crystallization/precipitation. Therefore, crystallization and precipitation are not suitable to recover FA/formate from dilute streams of an electrochemical reactor.

Other methods for FA separation either are related to one of the previous techniques (e.g., reactive distillation, salting-out extraction, supercritical fluid extraction, and adsorption) or have

a low potential/technology readiness level (TRL) for large-scale deployment (e.g., conventional membranes, liquid chromatography, and CO₂-switchable solvents).

In summary, the separation of FA or formate from aqueous solutions is a challenging task, especially when the concentrations are low, and the pH is larger than the pK_a of FA. Distillation, extraction, and ion-exchange resins cannot be used to separate the dissociated form of the acid (i.e., formate). Electrodialysis is an interesting option to concentrate and acidify formate solutions but suffer from efficiency loss at high concentrations and consequently a high power consumption. Crystallization and precipitation are not suitable for FA or formate separation because the concentration in the feed is too low and the solubility of formate salts in water is relatively high. The undissociated form of the acid (i.e., FA) can be separated by conventional distillation up to the azeotropic composition, but the low concentration of the high boiling FA will require an excessive amount of energy for water removal. Liquid–liquid extraction is currently the best technology to remove FA (i.e., the undissociated acid) from dilute streams. There is still a need for better extraction solvents with improved distribution coefficients, separation factors, and mutual solubilities.

Economics of CO₂ Electroreduction to Formic Acid/Formate. A commercial CO₂ electrolysis process will likely be accompanied by a range of supporting units like CO₂ capture, reactant recycling, and product recovery. A possible process scheme is shown in Figure 9. CO₂ is captured from biogas, flue gas, or air and fed to the electrolyzer, which uses (recycled) water and renewable energy from solar or wind to convert CO₂ to valuable products. In the following process steps, the unconverted reactants/electrolytes are recycled and the electroreduction products are separated using conventional methods. Depending on the product, concentration, and conversion, gas–gas, gas–liquid, liquid–liquid, or solid–liquid separations might be required. The techno-economic evaluation will include costs for CO₂ capture, CO₂ electrolysis, reactant recycling, and product separation. The cost estimates of all of these components involve some degree of uncertainty, which is related to the low technology readiness level (TRL) of the process. Therefore, we will perform a sensitivity analysis including a base case, an optimistic (best) case, and a pessimistic (worse) case scenario. In the following, the assumptions underlying the cost estimate of the major components will be discussed.

Cost of CO₂. The cost of CO₂ capture depends on the applied separation technology, the concentration of CO₂ in the mixture, and the source. A comprehensive review of CO₂ capture technologies can be found in several recent studies.^{126,127} Generally, it is more expensive to capture CO₂ from dilute streams like air or postcombustion flue gas than from more concentrated streams like biogas and precombustion flue gas. In fact, only very energy-intensive processes based on chemical solvents (e.g., amines) are suitable to capture CO₂ from dilute sources. Physical solvents are less energy demanding but can only be applied at sources (e.g., IGCC, biogas, and natural gas) with relatively high CO₂ partial pressures. In Table 3, an overview of the cost of CO₂ capture from different sources is provided. In the literature, the cost of CO₂ capture is reported in many different metrics, i.e., the cost of CO₂ avoided (COCA), the cost of CO₂ captured (COCC), the cost of CO₂ reduced/abated (COCR), and the increased cost of electricity (ICOE). All of these measures have a different meaning but bear a common unit (\$/ton CO₂), which can be confusing to

Table 3. Cost of CO₂ Captured (COCC) from Different Sources (All Values Are in 2013 U.S. Dollars, Unless Otherwise Mentioned)

source ^a	COCC (\$/ton CO ₂)
SCPC	36–53
NGCC	48–111
IGCC	28–41
oxy	36–67
biogas	25–50
natural gas	30–40
air	100–1000

^aSCPC, postcombustion capture at supercritical pulverized coal plants; NGCC, postcombustion capture at natural gas combined cycle plants; IGCC, precombustion capture at coal-based integrated gasification combined cycle plants; and oxy, oxy-combustion capture at SCPC plants. Data taken from refs 128–130, 132, and 133.

nonexperts. Here, the cost of CO₂ captured will be used, which excludes the cost of transportation and storage. For capture from flue gas and biogas, the cost ranges from \$30 to \$100/ton CO₂ captured. Recently, Rubin et al.¹²⁸ estimated the cost of CO₂ capture (between \$40 and \$60/ton of CO₂ captured) for the Boundary Dam plant in Canada and the Petra Nova plant in U.S., which are currently the only two commercial-scale coal-fired power plants in the world that use carbon capture and storage (CCS) technology. For direct air capture (DAC), the most recent cost estimate is between \$100 and \$230/ton CO₂, but much higher costs (\$500–1000/ton CO₂) have been stated in the past.^{129,130} For the base case, we will use a CO₂ price of \$50/ton, which falls within the cost range of CO₂ capture from biogas and flue gas. The amount of CO₂ required to produce a certain amount of FA/formate can be obtained from the reaction stoichiometry



Ideally, 1 mol FA requires 1 mol CO₂ and 2 mol protons and electrons. The actual amount of CO₂ required will be higher, since the single-pass conversion is not 100%. For a single-pass conversion of 50%, the amount of CO₂ required is twice the stoichiometric amount. For economic reasons, the unconverted CO₂ should be recycled. Therefore, an additional separation/recycling step for CO₂ will be required depending on the single-pass conversion of CO₂, the FE, and the byproducts in the electrolyzer. The single-pass conversion is often <50%, which means that a large fraction of the supplied CO₂ leaves the reactor without being converted.^{37,131} This is not an issue for a high FE, since the unconverted CO₂ can simply be recycled. However, for a low FE, the byproducts (e.g., CO and H₂) might mix (or not depending on the cell design) with the unconverted CO₂ stream. This stream can be purged for high conversions and FEs but requires recycling for low conversions and byproduct recovery for low FEs. Since the FE of CO₂ conversion to FA is relatively high (>90%), the partial pressure of CO₂ in the recycle stream will be high. For this reason, physical solvents/adsorbents can be used for CO₂ capture and recycling. The byproducts (<10%) can be obtained in high purities because the solubility/adsorption of CO/H₂ in/on physical solvents/adsorbents is low. Here, pressure-swing adsorption (PSA) with activated carbon will be used for CO₂ capture and recycling. The capital and operating costs for recycling the unconverted CO₂ are roughly the same as the cost of CO₂ capture from biogas or natural gas (\$40/ton). Therefore, a CO₂ electrolyzer that

operates at low conversions will significantly increase the cost of CO₂ capture and recycling. In Table 4, the effect of CO₂

Table 4. Effect of Conversion on the Economics of CO₂ Capture and Recycling

case	ideal	best	base	worse
conversion	1	0.75	0.5	0.25
CO ₂ required (kg/h)	478	637	955	1911
CO ₂ required (ton CO ₂ /ton FA)	0.96	1.27	1.91	3.82
CO ₂ recycling (kg/h)	0	159	478	1433
CO ₂ recycling (ton CO ₂ /ton FA)	0	0.32	0.96	2.87
price of CO ₂ capture (\$/ton CO ₂)	0	25	50	100
price of CO ₂ recycling (\$/ton CO ₂)	0	20	40	80
cost of CO ₂ (\$/ton FA)	0	32	96	382
cost of CO ₂ recycling (\$/ton FA)	0	6	38	229
total cost of CO ₂ (\$/ton FA)	0	38	134	611

conversion on the economics of CO₂ capture and recycling is presented. At 100% conversion, the amount of CO₂ required to produce 500 kg/h of FA is around 478 kg/h and no recycling is needed. However, at a conversion of 25%, not only the amount of CO₂ required is 4 times higher (1911 kg/h), but 75% of this (i.e., 1433 kg/h) needs to be recycled as well. It is clear that a low conversion will add significant expenses for recycling CO₂. For the best, base, and worse case scenarios, conversions of 75, 50, and 25% will be assumed, respectively.

Cost of Electricity. For electrochemical processes, the consumption of electricity has a large contribution to the total production cost. Therefore, the price of electricity will have a significant impact on the economics of CO₂ electroreduction. The intermittent behavior of renewable energy causes huge fluctuations in the electricity price, which can be negative in some cases. Furthermore, the cost of renewable energy depends on the source type (solar or wind), capacity, region, season, demand, market, policy, and so on. It is therefore difficult to accurately predict the (future) price of renewable electricity. Due to its simplicity, the levelized cost of electricity (LCOE) is often used as a metric to compare the performance of different (renewable and nonrenewable) technologies, but the method has some inherent well-known drawbacks. A sensitivity analysis will be performed to take into account the uncertainty in the LCOE from renewables. As input for the three scenarios, the current and the anticipated future LCOE in Europe (in particular Germany) will be used. Here, the main focus is on the LCOE from solar and wind, since other sources like hydro and geothermal are restricted to countries with a strategic geographical location. The (future) LCOE from renewable energy sources has been analyzed in some detail by McKinsey & Company, Lazard, IRENA, IEA, and Fraunhofer.^{134–138} The current LCOE of onshore wind and solar photovoltaic (PV) is in the range of \$40–60/MWh, which is expected to nearly halve by 2030. For the base case, we will assume an electricity price of \$50/MWh.

Capital and Operating Costs of the CO₂ Electrolyzer. Current estimates for the cost of CO₂ electrolyzers are subjected to large uncertainties due to the lack of commercial-scale applications. A first estimate of the cost can be obtained by comparison with similar commercial-scale processes like hydrogen or chlor-alkali production from water or brine electrolysis, respectively. The capital cost of CO₂ electrolyzers will be deduced from these two well-established electrochemical processes. In Table 5, an estimate of the capital costs for alkaline

Table 5. Estimated Capital Costs of Hydrogen, Chlor-Alkali, and CO₂ Electrolyzers

parameter	unit	AEC ^a	chlor-alkali	CO ₂ -EC
cell voltage	V	1.75	3	3
CD	mA/cm ²	300	500	200
power	kW/m ²	5.3	15	6
CAPEX ^b	€/kW	1000	2000	5000
CAPEX	€/m ²	5250	30 000	30 000

^aAlkaline electrolysis cells for hydrogen production. ^bFor simplicity, an euro to dollar exchange rate of 1 will be used.

hydrogen electrolysis cells (AECs), chlor-alkali membrane cells, and CO₂ electrolyzers is provided. The CAPEX of €1000/kW (~€5250/m²) for AEC is taken from Schmidt et al.,¹³⁹ which can be compared with the values used by Jouny et al.¹⁹ (~\$1000/m²) for alkaline electrolyzers and by Spurgeon et al.²⁰ (~\$30 000/m²) for proton-exchange membrane (PEM) electrolyzers. The CAPEX of the chlor-alkali process is around \$200 000–\$300 000/ton per day chlorine capacity, which is in agreement with the investment cost of \$411 million for a recent Dow–Mitsui chlor-alkali plant with a capacity of 800 000 ton/year.^{140–142} Using typical values for the cell voltage and CD, the CAPEX of chlor-alkali electrolyzers per unit of power input can be estimated to be around \$2000/kW.¹⁴³ For the base case, we have assumed that the capital cost of the CO₂ electrolyzer per unit area is similar to that of the chlor-alkali process (~\$30 000/m²). This is a factor 30 higher than the value used by Jouny et al.¹⁹ but similar to the base-case value of Spurgeon et al.²⁰ However, we believe that this cost of merit is reasonable considering the complexity of (GDE-based) CO₂ electrolyzers and the similar operating range (CD and potential) as the chlor-alkali process.

The operating cost of the CO₂ electrolyzer is mainly determined by the power consumption (P in watts), for a given capacity (C in kilogram of FA)

$$\frac{P}{C} = \frac{V \cdot n \cdot F}{t \cdot M_w \cdot FE} \quad (11)$$

where V is the cell voltage, n is the number of electrons (2 for FA), F is the Faraday constant (C/mol), t is the time (s), M_w is the molecular weight of FA (kg/mol), and FE is the Faraday efficiency of FA. In Tables 6 and 7, an estimate of the capital and

Table 6. Estimated Capital and Operating Costs of a CO₂ Electrolyzer for 500 kg/h Formic Acid Production^a

case	best	base	worse
cell voltage (V)	2	2.5	3.5
CD (mA/cm ²)	200	200	200
FE (%)	90	80	70
electricity (\$/MWh)	25	50	100
electrolyzer area (m ²)	324	364	416
CAPEX (\$/m ²)	15 000	30 000	60 000
CAPEX (M\$)	4.9	10.9	25.0
CAPEX (\$/kg FA)	0.081	0.182	0.416
OPEX (k\$/year)	259	727	2327
OPEX (\$/kg FA)	0.065	0.182	0.582
CAPEX + OPEX (\$/kg FA)	0.146	0.364	0.998

^aEconomic analysis is based on a plant capacity of 500 kg/h, a lifetime of 15 years, and 8000 h/year of operation. Maintenance, depreciation, interest, and taxes are excluded.

Table 7. Estimated Capital and Operating Costs of a CO₂ Electrolyzer for 500 kg/h Formate Production^a

case	best	base	worse
cell voltage (V)	2	2.5	3.5
CD (mA/cm ²)	250	250	250
FE (%)	95	90	75
electricity (\$/MWh)	25	50	100
electrolyzer area (m ²)	245	259	311
CAPEX (\$/m ²)	15 000	30 000	60 000
CAPEX (M\$)	3.7	7.8	18.6
CAPEX (\$/kg FA)	0.061	0.129	0.311
OPEX (k\$/year)	245	646	2172
OPEX (\$/kg FA)	0.061	0.162	0.543
CAPEX + OPEX (\$/kg FA)	0.123	0.291	0.854

^aEconomic analysis is based on a plant capacity of 500 kg/h, a lifetime of 15 years, and 8000 h/year of operation. Maintenance, depreciation, interest, and taxes are excluded.

operating costs of a CO₂ electrolyzer with a capacity of 500 kg/h for formic acid and formate is provided. For the base case of the FA route, a cell voltage of 2.5 V, CD of 200 mA/cm², FE of 80%, and electricity price of \$50/MWh were assumed. For the base case of the formate route, a cell voltage of 2.5 V, CD of 250 mA/cm², FE of 90%, and electricity price of \$50/MWh were assumed. Under these conditions, the cost of producing 1 ton of formic acid and formate is \$364 and \$291, respectively. In the best case, the cost reduces to ~\$146 and \$123 for FA and formate, respectively.

Cost of Downstream Separation. As discussed earlier, the downstream process for FA separation depends on the dissociation state of the acid. Liquid–liquid extraction has been selected to remove the molecular (undissociated) form of the acid from dilute streams at low pH conditions. In Figure 10, a simplified process scheme for the extraction of FA with a low boiling solvent, which forms a low boiling azeotrope with water, is shown. For the extraction of FA, 2-MTHF was selected. A dilute FA stream from the electrolyzer is fed at the top of the extractor, which uses a low boiling solvent (i.e., 2-MTHF) to selectively extract the acid from the aqueous phase. The extract containing water, solvent, and FA is introduced into the azeotropic distillation column. The low boiling heterogeneous solvent–water azeotrope is recovered as tops, while the bottom stream contains around 75 wt % FA, which is free of 2-MTHF. This stream is introduced into a vacuum distillation column to obtain at least 85 wt % of FA. The heterogeneous solvent–water azeotrope is split in a decanter-type condenser into two liquid streams. The solvent-rich phase is partly refluxed to the azeotropic distillation column and partly recycled to the extractor. The water-rich phase and the raffinate stream from the extractor require some treatment to prevent solvent loss and to comply with environmental regulations. A steam stripper supported with a decanter is used to recover the low boiling solvent, which is recycled to the extractor. The purified water stream from the stripper can be recycled to the electrolyzer. Heat integration between the units and solvent reclamation steps to clean the recycled solvent were not considered in the process design and economic analysis. The process shown in Figure 10 was modeled with Aspen Plus to estimate the capital and utility costs. For the base case, a feed mass flow rate to the extractor of 5000 kg/h with 10 wt % of FA in water was assumed. The effect of electrolytes on the separation performance of the extraction unit and the distillation column was neglected. The presence of

salts is often beneficial for the extraction of FA due to a salting-out of water from the organic phase, which increases the separation factor of FA. These effects are challenging to capture in a simulation because of the requirement of an accurate electrolyte model. However, such a technical detail is of minor importance at the conceptual process design stage and has been ignored. The most crucial step is the selection of an adequate model in Aspen Plus to correctly represent the phase behavior of the mixtures. The selected model should be validated against experimental data [e.g., VLE, LLE, vapor–liquid–liquid equilibrium (VLLE), and azeotrope formation]. Models that fail to reproduce the phase behavior or produce a spurious azeotrope should be discarded immediately, since it will directly influence the performance, sizing, and costs of the separation units. For associating systems, the Aspen manual recommends the use of the UNIQUAC and NRTL activity coefficient models for the liquid phase and the Hayden–O’Connell (HOC) model to account for the dimerization in the vapor phase. For the selected models, the binary and ternary phase diagrams of the solvent–FA–water system were computed and compared with available experimental data. The results show that the NRTL-HOC model performs better than the UNIQUAC-HOC model in representing the experimental VLE data of water and FA. The experimental LLE data of Glass et al.¹⁴⁴ was used to fit the NRTL parameters of the 2-MTHF–water system. The NRTL parameters for the 2-MTHF–FA system were fitted to the azeotropic data of Hangx et al.⁷⁸ All other parameters were taken from the Aspen databank. The validation of modeling results can be found in the [Supporting Information](#).

After selecting the correct model, the process flow diagrams were developed and simulated in Aspen Plus. The extraction and distillation columns were, respectively, modeled with the EXTRACT and RADFRAC unit operation blocks of Aspen Plus. It is now a matter of optimizing the units to meet the design/separation specifications using a minimum of energy input. For extraction columns, a general guideline is to set the extraction factor (E') between 1.5 and 2. The extraction factor is defined as

$$E' = K_B \frac{S'}{F'} \quad (12)$$

where K_B is the partition ratio in Bancroft coordinates and S'/F' is the solvent-to-feed ratio. The extraction column can be optimized by calculating different combinations of solvent flow rates and the required number of stages to meet the design specification. The optimal design was one that achieved 99.5% FA recovery with a minimal number of stages with the constraint that the extraction factor should be between 1.5 and 2. The fractional recovery of FA was calculated as the ratio of the FA mass flow of the extract and feed streams. For the design of the azeotropic distillation column, the bottom stream should contain at least 75 wt % FA and less than 0.005 wt % of the extraction solvent with the remainder being water, while the loss of FA through the tops should be at most 0.005 wt %. Note that the residue will contain a mixture of FA and water, since significant amounts of water are coextracted in the extraction column. The vacuum distillation column was designed to produce at least 85 wt % of FA as tops. The distillation columns were optimized in Aspen Plus using the built-in Model Analysis tool. For a given number of stages and design constraints/specifications, the reflux ratio and the location of the feed stage were optimized by minimizing the condenser and reboiler duties. A similar optimization strategy was used for the design of

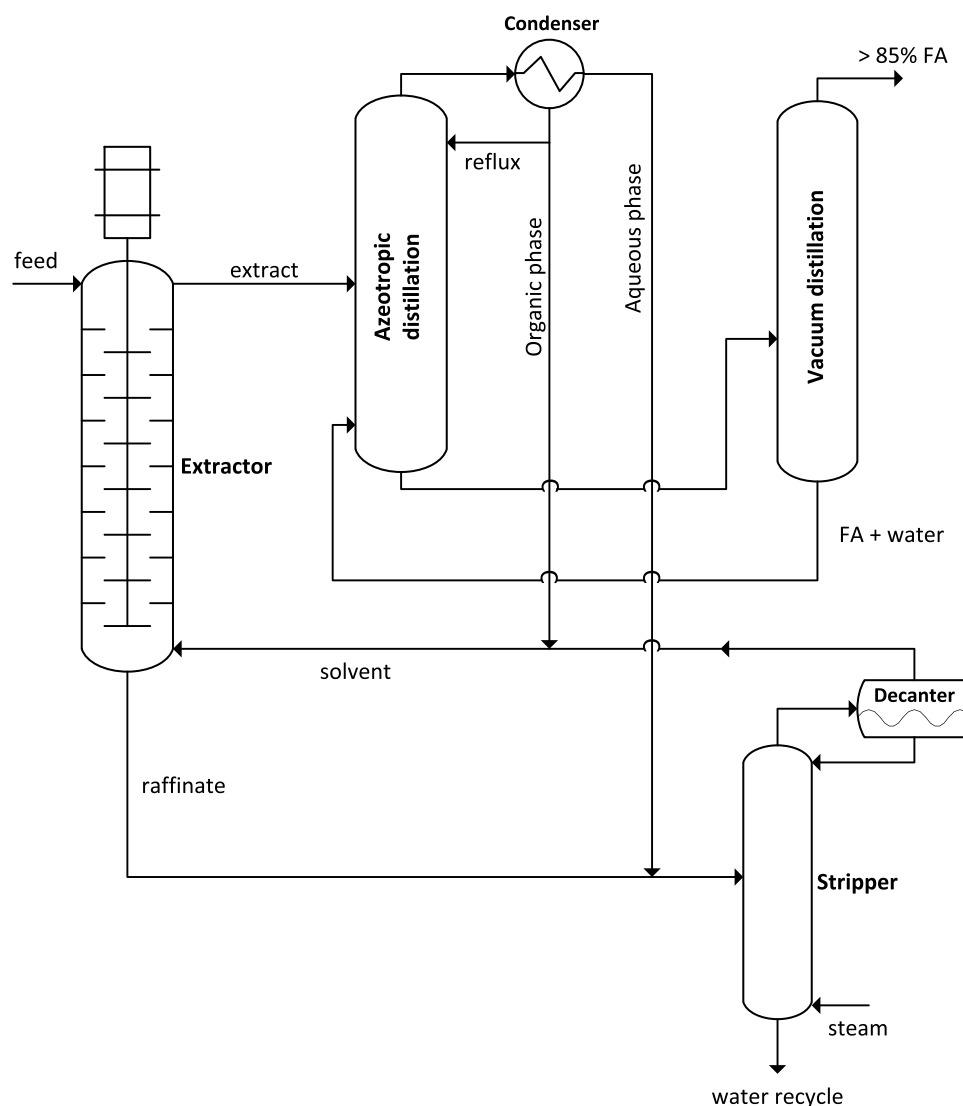


Figure 10. Simplified diagram to extract FA with a low boiling solvent, which forms a low boiling heterogeneous azeotrope with water. A dilute stream of FA from the electrolyzer is fed to the extraction column, which uses a low boiling solvent (e.g., 2-MTHF) to remove FA from water. The extract is sent to the azeotropic distillation column to recover the solvent–water azeotrope as tops and the product (~75 wt % FA) as bottoms. The heterogeneous solvent–water azeotrope is split into two liquid streams in a decanter-type condenser. The organic-rich phase containing the solvent is partly refluxed to the distillation column and partly recycled to the extractor. The water-rich phase is, after combining with the raffinate from the extractor, sent to the stripper. The bottom stream from the azeotropic distillation column is sent to the vacuum distillation column to obtain a more concentrated (>85 wt %) FA stream as the distillate. The bottom stream of the vacuum distillation column is recycled to the azeotropic distillation column. The raffinate is stripped with steam to recover small amounts of solvents dissolved in water. The low boiling solvent–water heterogeneous azeotrope is condensed and split into two liquid streams. The light phase containing the solvent is recycled to the extractor, while the heavy phase is refluxed to the stripper. Water leaving the stripper can be recycled to the electrolyzer.

the steam stripper for raffinate treatment. The design that used the minimum number of stages and steam consumption to obtain a water purity of 99.95 wt % was adopted. The distillation columns were sized using the Tray Sizing tool in Aspen Plus. The tray efficiencies of the extraction and distillation columns were set to 25 and 75%, respectively. The scale-up/sizing of extraction columns is not trivial, since it is common practice to first run pilot plant tests before large-scale application. Here, the empirical equations of Todd et al.¹⁴⁵ were used to size the extractor; see the [Supporting Information](#) for details. The capital cost of the extractor was obtained from the correlations in the book of Woods.¹⁴⁶ The operating costs of extractors are typically very small (<3%) compared with the solvent recovery units. Here, we have assumed that the operating cost of the extraction unit is 3% of the total operating cost of the process shown in

Figure 10. The decanter to separate the heterogeneous water–solvent azeotrope into two immiscible liquid streams was modeled with the in-built condenser/decanter model of RADFRAC in Aspen Plus. The capital and utility costs for the hybrid extraction–distillation process can be found in [Table 8](#). The cost of concentrating 10 wt % FA to 85 wt % is around \$245/ton. We note that the contribution of the capital cost to the total cost is almost half, which is due to the relatively small scale (500 kg/h) of the process. Furthermore, a cost breakdown shows that the extractor has only minor contributions to the total cost. The major costs come from the solvent recovery units (i.e., distillation and stripping), which is typical for extraction processes. Recently, Hidajat et al.^{147–149} estimated the economics of the BASF and the Kemira–Leonard process for formic acid production. The cost of FA separation for the BASF

Table 8. Cost Estimation of the Hybrid Extraction–Distillation Process^a

unit	extraction	solvent recovery	total
CAPEX (k\$)	750	7000	7750
CAPEX (\$/kg FA)	0.013	0.117	0.129
OPEX (k\$/year)	14	450	464
OPEX (\$/kg FA)	0.004	0.113	0.116
total (\$/kg FA)	0.016	0.229	0.245

^aEconomic analysis is based on a plant capacity of 500 kg/h, a lifetime of 15 years, and 8000 h/year of operation. Maintenance, depreciation, interest, and taxes are excluded.

process, which is also based on liquid–liquid extraction, was estimated to be around \$115/ton. The cost of FA separation for the Kemira–Leonard process, which is based on pressure-swing distillation, was estimated to be around \$145/ton. The difference of around \$100/ton between our cost estimate for FA separation and that of Hidajat et al. is mainly due to the (6 times) larger scale of their process (i.e., the capital cost). Furthermore, we neglected heat integration, while the process of Hidajat et al.¹⁴⁹ was fully optimized and heat integrated.

The separation, concentration, and acidification of dilute formate solutions (i.e., the dissociated form of the acid at high pH conditions) are more challenging. We have selected electro dialysis with bipolar membranes to acidify and concentrate formate solutions because conventional methods do not concentrate the stream and produce undesired salts upon addition of acids. Furthermore, the presence of acids will catalyze esterification reactions in the distillation column when alcohols are used in the preceding extraction step. For these reasons, a combination of electro dialysis and distillation is used to obtain a concentrated FA product from dilute formate streams; see Figure 11. The feed containing 10 wt % potassium

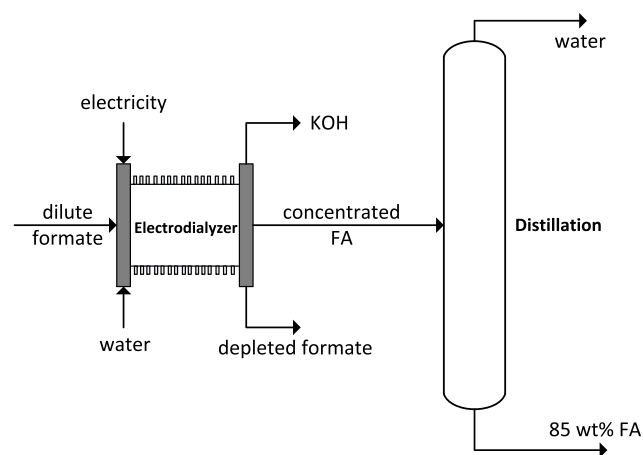


Figure 11. Simplified process diagram to convert formate to FA with a bipolar membrane electro dialyzer. Conventional distillation at elevated pressure (around 4 bar) is used to obtain an azeotropic mixture of 85 wt % FA and water.

formate is fed to the electro dialyzer, which uses a bipolar membrane in a three-compartment configuration to convert the formate salt into formic acid and potassium hydroxide. The solution is only concentrated up to 30 wt % FA to prevent product crossover and efficiency loss at higher concentrations. This concentrated stream is sent to the distillation column, which is operated at a pressure of 4 bar, resulting in an azeotropic

mixture of around 85 wt % FA and water as bottoms. Water leaving the distillation column as tops can be recycled to the electro dialyzer. Here, heat integration and salt effects on the distillation performance were neglected. For higher FA concentrations, at least one additional distillation column will be required. Optionally, one can use the previously explained extraction followed by the distillation process to reach higher concentrations, but this will increase the cost significantly.

The capital and utility costs of the electro dialyzer were obtained by scaling up the experimental results of Jaime Ferrer et al.^{121,122,120} for the BPM-based three-compartment cell. The capital costs of electro dialysis processes are mainly determined by the required membrane area for a given capacity. The required membrane area (A) can be computed from

$$A = \frac{nFQ_{st}(C^f - C^d)}{i\zeta} \quad (13)$$

where n is the electrochemical valence of formate, F is the Faraday constant (C/mol), Q_{st} is the volume flow (L/s) in the stack, i is the current density (A/m²), ζ is the current efficiency, and C^f and C^d are the concentrations of FA in the feed and diluate stream (mol equiv/L), respectively. We have assumed that the diluate stream is free of formic acid. It is important to note that the current efficiency in electro dialysis processes is a strong function of the CD and the concentration of the acids and/or bases. The cost of the stack and peripheral equipment is taken as a fraction of the membrane cost. The operating cost is dominated by the power consumption of the stack and the peripheral equipment. The power consumption of the BPM-AEM-CEM stack (E^{st}) was reported by Jaime-Ferrer et al.¹²⁰ to be around 2.5 kWh/kg of FA at a CD of 50 mA/cm² and an FA concentration of 7 mol/L. The energy consumption of the peripheral equipment is taken as 5% of E^{st} . The capital and utility costs of the distillation unit were obtained from the Aspen Process Economic Analyzer. In Table 9, an overview of the capital and operating costs of the electro dialyzer and distillation process is provided. The results show that the cost of conversion and concentration of formate to FA up to 30 wt % is around \$190/ton of FA. The distillation process to obtain 85 wt % FA adds another \$190/ton to the cost. Therefore, the total cost to convert 10 wt % formate to 30 wt % FA, which is subsequently concentrated up to 85 wt %, is around \$380/ton of FA. The downstream separation costs in the best and worse case scenarios are \$240 and \$630/ton of FA, respectively.

Economic Analysis of the Supply Chain. Now that the costs of all of the components are known, an economic analysis of the whole supply chain (from CO₂ capture to conversion to downstream separation of products) can be performed. The economic analysis will be performed for two cases: (a) CO₂ electroreduction to formate and subsequent conversion to 85 wt % FA (indirect conversion) and (b) CO₂ electroreduction to formic acid and subsequent concentration to 85 wt % FA (direct conversion). In Tables 10 and 11, an overview of the costs of electrochemical CO₂ conversion to formate and formic acid, including CO₂ capture/recycling, electrochemical conversion, and product separation, is provided. In the base case, the costs of producing 1 ton of FA through the indirect and direct routes are around \$803 and \$743, respectively. Note that these costs are reported on the basis of 1 ton of pure FA. The costs for 85 wt % FA are around \$683 and \$631 for the indirect and direct routes, respectively. Taking into account the accuracy of the cost estimates ($\pm 30\%$), both routes have the same economic

Table 9. Estimated Downstream Separation Costs of Converting 10% Formate to 85 wt % FA^a

case	best	base	worse
electrodialysis			
electrolyte feed (kg/h)	5000	5000	5000
FA concentration in (w/w)	0.1	0.1	0.1
FA concentration out (w/w)	0.3	0.3	0.3
power (kWh/kg)	1.5	2.5	4
electricity price (\$/MWh)	25	50	100
CD (A/m ²)	1000	500	500
current efficiency	0.95	0.75	0.6
membrane area (m ²)	292	740	925
cost BPM (\$/m ²)	500	1000	1000
cost AEM (\$/m ²)	150	150	150
cost CEM (\$/m ²)	150	150	150
membrane cost (k\$)	234	962	1202
stack cost (k\$) ^b	351	1443	1804
peripheral equipment (k\$) ^c	526	2164	2706
total investment (k\$)	876	3607	4509
CAPEX (\$/kg)	0.01	0.06	0.08
OPEX (\$/kg)	0.04	0.13	0.37
total cost electrolysizer (\$/kg)	0.05	0.19	0.44
distillation			
capacity (kg/h of FA)	500	500	500
FA concentration in (w/w)	0.3	0.3	0.3
FA concentration out (w/w)	0.85	0.85	0.85
CAPEX (\$/kg)	0.06	0.06	0.06
OPEX (\$/kg)	0.12	0.12	0.12
total cost distillation (\$/kg)	0.19	0.19	0.19
total cost (\$/kg of FA)	0.24	0.38	0.63

^aEconomic analysis is based on a lifetime of 15 years and 8000 h/year of operation. Maintenance, depreciation, interest, and taxes are excluded. ^bStack cost is 1.5 times the membrane cost. ^cPeripheral equipment cost is 1.5 times the stack cost.

Table 10. Estimated Cost of Electrochemical Reduction of CO₂ to Formate and Subsequent Conversion to 85 wt % FA^a

case	best	base	worse
cost CO ₂ capture (\$/ton FA)	32	96	382
cost CO ₂ recycling (\$/ton FA)	6	38	229
CO ₂ conversion (\$/ton FA)	123	291	854
downstream (\$/ton FA)	241	378	630
total cost (\$/ton FA)	402	803	2095

^aEconomic analysis is based on a lifetime of 15 years and 8000 h/year of operation. Maintenance, depreciation, interest, and taxes are excluded.

Table 11. Estimated Cost of Electrochemical Reduction of CO₂ to 85 wt % FA^a

case	best	base	worse
cost CO ₂ capture (\$/ton FA)	32	96	382
cost CO ₂ recycling (\$/ton FA)	6	38	229
CO ₂ conversion (\$/ton FA)	146	364	998
downstream (\$/ton FA)	123	245	490
total cost (\$/ton FA)	306	743	2100

^aEconomic analysis is based on a lifetime of 15 years and 8000 h/year of operation. Maintenance, depreciation, interest, and taxes are excluded.

viability. The indirect route mainly relies on the availability of cheap electricity and membranes to run the electrolysizer. In

contrast, the economics of the direct route strongly depends on the formic acid concentration in the feed; see the [Supporting Information](#). Therefore, the direct route of producing FA is more interesting if higher FA concentrations can be achieved in the electrochemical cell. We note that concentrations up to ~50 wt % FA have already been obtained but at a relatively low FE or CD.³⁸ The economics of the FA process will improve significantly if the cause of the FE reduction at such high concentrations can be resolved. In the best case, the costs reduce to around \$400 and \$300/ton of FA for the indirect and direct routes, respectively. Considering the market price of 85 wt % FA (\$600–\$800/ton), both routes of producing FA can be profitable, but the direct route is slightly more interesting. To increase the margins, many different aspects of the electrochemical CO₂ conversion process need to be improved. In the following, a list of challenges is presented that will have a significant impact on the economics of electrochemical CO₂ reduction processes.

Challenges and Opportunities. To improve the economics of CO₂ electroreduction to valuable (liquid) products, many hurdles need to be overcome. In [Table 12](#), an overview of the

Table 12. Challenges and Opportunities to Improve the Economics of CO₂ Electroreduction to Valuable Products

components	opportunities
electrodes	development of (acid) stable high-lifetime electrodes with low overpotential for the redox reactions
membranes	development of membranes with low ohmic resistance and product crossover/leakage
anodic reaction	search for an alternative reaction, instead of OER, to produce a more valuable product at the anode
electrolytes	minimize the use of electrolytes (e.g., catholyte-free electrolysis) to avoid difficult separations
conversion	strategy for high single-pass conversion is desired to minimize gas separation
solvents	use of nonaqueous solvents will facilitate easier separation of (polar) products
flow	optimize gaseous or liquid flows to avoid mass transfer limitations and to concentrate products
efficiency	synergy between all reactor components is required to obtain high FE and CD at low cell potentials
separation	products should be obtained in high concentrations to minimize downstream separation costs

components that will have a significant impact on the process economics of CO₂ electroreduction is provided. Electrodes need to be developed with a low overpotential for the reduction and oxidation (redox) reactions, a high stability in alkaline and acidic environments, and a high lifetime. For weak acids like FA or acetic acid, it is desired to develop stable catalysts that can operate in acidic media without affecting the product selectivity. This will eliminate the requirement of an acidification step downstream of the process. Membranes with a low resistance, high product rejection, and high fouling resistance are required. Currently, achieving high FA concentrations (>10 wt %) at high FEs and CDs is limited by product crossover through membranes and the transport of concentrated products, which can block the supply of CO₂ molecules to the cathode.^{38,57} The use of electrolytes should be minimized to avoid downstream separation issues. In this regard, catholyte-free CO₂ electrolysis as reported by Lee et al.⁵⁷ or solid electrolytes (e.g., the ion-exchange resins used by Yang et al.⁵⁴ or the proton/formate conducting solid electrolyte by Xia et al.³⁸) that do not contaminate the product should be preferred. Furthermore, the

use of excessive electrolytes will cause solid formation in an FA distillation column. At pressures higher than 1 bar, water will leave the column as a distillate, while FA and the electrolytes are concentrated in the bottoms, which will cause precipitation of the salts. The use of nonaqueous solvents will not only increase the CO₂ solubility but also facilitate easier separation of dilute (polar) products like carboxylic acids and alcohols. By carefully selecting a nonaqueous solvent, the products can be in situ extracted in the electrolyzer avoiding a downstream extraction step. The flow and contacting time of reactants and products should be optimized to minimize mass transfer limitations, allow high single-pass conversion, and obtain products in high concentrations. Low single-pass conversion and dilute product streams will require expensive gas–gas, gas–liquid, or liquid–liquid separations. Synergy between all reactor components is essential to obtain high efficiencies and current densities at low cell potentials. Separation should be considered in an early stage of the reactor design. The works of Yang et al.⁵⁴ and Xia et al.³⁸ clearly demonstrate the concept of downstream simplification by design. One should a priori avoid difficult-to-separate mixtures involving excessive electrolytes, dilute (polar) product streams, unconverted reactants, and weak acids at pH > pK_a. Electrochemists should not only aim for a high FE and CD at a low overpotential, but a high (liquid) product concentration is equally important from an economic point of view. Without a good strategy for downstream separation of (dilute) products, the (photo)electrochemical reduction of CO₂ to chemicals and fuels will suffer the same fate as the fermentation process. An alternative reaction at the anode, instead of the OER, which either requires a lower overpotential or produces a more valuable product than oxygen, will significantly improve the overall economics of the electrolyzer. The coelectrolysis of CO₂ and glycerol reported by Verma et al.¹⁵⁰ is an example of this strategy. However, such an integration might require a redesign of the reactor/catalyst to optimize the conditions of both reactions, prevent crossover/mixing of anodic and cathodic products, and for recovery of both products. It is clear that many different aspects of the electrochemical CO₂ reduction process need to be improved before commercialization.

CONCLUSIONS

A high-pressure semicontinuous batch electrolyzer with a tin-based cathode was used to convert CO₂ in acidic media to formic acid. The effects of CO₂ pressure, bipolar membranes, and electrolyte concentration on the Faraday efficiency (FE) of formic acid (FA) and the current density (CD) were investigated. The results show that at high pressures it is possible to efficiently convert CO₂ to formic acid (i.e., the molecular form of the acid) at low pH conditions. The highest FE (~80%) was obtained at a pressure of 50 bar at a cell potential of 3.5 V and a CD of ~30 mA/cm². The FE of FA in alkaline media is higher (~90%) but produces formate (i.e., the ionic form) instead of formic acid. We show that the minor difference between the two forms of FA has major consequences for the downstream separation process. Distillation, extraction, adsorption with ion-exchange resins, electrodialysis, and crystallization/precipitation have been reviewed for FA/formate purification from dilute streams of the CO₂ electrolyzer. Using process heuristics, liquid–liquid extraction and electrodialysis with bipolar membranes have been selected to recover/concentrate FA and formate, respectively. A techno-economic analysis of the electrochemical reduction of CO₂ to FA or formate has been performed. This analysis included the costs of

CO₂ capture, electrochemical conversion to FA/formate, recycling of unconverted CO₂, and downstream separation. We demonstrate that FA is economically a more attractive product than formate, even when an FE penalty of 10% for FA in the CO₂ electrolyzer is considered. In addition to a high Faraday efficiency and current density at low overpotentials, electrochemists should also aim for a high product concentration and single-pass conversion. The results reported here urge for a better design of CO₂ electrocatalysts that can operate at low pH conditions without affecting the selectivity of the desired products and technologies for efficient separation of dilute products from (photo)electrochemical reactors.

ASSOCIATED CONTENT

Supporting Information

The Supporting Information is available free of charge at <https://pubs.acs.org/doi/10.1021/acs.iecr.9b03970>.

Compilation of distribution coefficient data of formic acid in chemical and physical solvents, selection of solvents, properties of formic acid and formate, sizing of the extractor, validation of modeling results with experimental data, and a plot of capital and operating costs of formic acid distillation as a function of feed concentration (PDF)

AUTHOR INFORMATION

Corresponding Author

*E-mail: t.j.h.vlugt@tudelft.nl.

ORCID

Mahinder Ramdin: 0000-0002-8476-7035

J. P. Martin Trusler: 0000-0002-6403-2488

Thijs J. H. Vlugt: 0000-0003-3059-8712

Notes

The authors declare the following competing financial interest(s): Coval Energy BV is developing a commercial process for the electrochemical conversion of carbon dioxide to formic acid.

ACKNOWLEDGMENTS

The authors thank Michel van den Brink for his help with the Ion-Chromatograph. The project [TEEI16076: Direct electrochemical conversion of CO₂ to formic acid (P2FA)] is being carried out with subsidy from the Dutch Ministry of Economic Affairs, under the scheme Joint Industry Projects, executed by Rijksdienst voor Ondernemend Nederland (RVO). T.J.H.V. acknowledges NWO-CW (Chemical Sciences) for a VICI grant.

REFERENCES

- (1) Gattrell, M.; Gupta, N.; Co, A. Electrochemical reduction of CO₂ to hydrocarbons to store renewable electrical energy and upgrade biogas. *Energy Convers. Manage.* **2007**, *48*, 1255–1265.
- (2) Sternberg, A.; Bardow, A. Power-to-What? - Environmental assessment of energy storage systems. *Energy Environ. Sci.* **2015**, *8*, 389–400.
- (3) Bushuyev, O. S.; De Luna, P.; Dinh, C. T.; Tao, L.; Saur, G.; van de Lagemaat, J.; Kelley, S. O.; Sargent, E. H. What Should We Make with CO₂ and How Can We Make It? *Joule* **2018**, *2*, 825–832.
- (4) De Luna, P.; Hahn, C.; Higgins, D.; Jaffer, S. A.; Jaramillo, T. F.; Sargent, E. H. What would it take for renewably powered electrosynthesis to displace petrochemical processes? *Science* **2019**, *364*, No. eaav3506.
- (5) Seh, Z. W.; Kibsgaard, J.; Dickens, C. F.; Chorkendorff, I.; Nørskov, J. K.; Jaramillo, T. F. Combining theory and experiment in

electrocatalysis: Insights into materials design. *Science* **2017**, *355*, No. eaad4998.

(6) Dinh, C.-T.; Burdyny, T.; Kibria, M. G.; Seifitokaldani, A.; Gabardo, C. M.; Garcia de Arquer, F. P.; Kiani, A.; Edwards, J. P.; De Luna, P.; Bushuyev, O. S.; Zou, C.; Quintero-Bermudez, R.; Pang, Y.; Sinton, D.; Sargent, E. H. CO₂ electroreduction to ethylene via hydroxide-mediated copper catalysis at an abrupt interface. *Science* **2018**, *360*, 783–787.

(7) Chen, C.; Khosrowabadi Kotyk, J. F.; Sheehan, S. W. Progress toward Commercial Application of Electrochemical Carbon Dioxide Reduction. *Chem* **2018**, *4*, 2571–2586.

(8) Kibria, M. G.; Edwards, J. P.; Gabardo, C. M.; Dinh, C.-t.; Seifitokaldani, A.; Sinton, D.; Sargent, E. H. Electrochemical CO₂ Reduction into Chemical Feedstocks: From Mechanistic Electrocatalysis Models to System Design. *Adv. Mater.* **2019**, No. 1807166.

(9) Song, J.; Song, H.; Kim, B.; Oh, J. Towards Higher Rate Electrochemical CO₂ Conversion: From Liquid-Phase to Gas-Phase Systems. *Catalysts* **2019**, *9*, No. 224.

(10) Jhong, H.-R. M.; Ma, S.; Kenis, P. J. Electrochemical conversion of CO₂ to useful chemicals: current status, remaining challenges, and future opportunities. *Curr. Opin. Chem. Eng.* **2013**, *2*, 191–199.

(11) Hori, Y. In *Solar to Chemical Energy Conversion*; Sugiyama, M., Fujii, K., Nakamura, S., Eds.; Springer International Publishing: Cham, 2016; Vol. 32, pp 191–211.

(12) Whipple, D. T.; Kenis, P. J. A. Prospects of CO₂ Utilization via Direct Heterogeneous Electrochemical Reduction. *J. Phys. Chem. Lett.* **2010**, *1*, 3451–3458.

(13) Lu, X.; Leung, D. Y. C.; Wang, H.; Leung, M. K. H.; Xuan, J. Electrochemical Reduction of Carbon Dioxide to Formic Acid. *ChemElectroChem* **2014**, *1*, 836–849.

(14) Kortlever, R.; Shen, J.; Schouten, K. J. P.; Calle-Vallejo, F.; Koper, M. T. M. Catalysts and Reaction Pathways for the Electrochemical Reduction of Carbon Dioxide. *J. Phys. Chem. Lett.* **2015**, *6*, 4073–4082.

(15) Vennekoetter, J.-b.; Sengpiel, R.; Wessling, M. Beyond the catalyst: How electrode and reactor design determine the product spectrum during electrochemical CO₂ reduction. *Chem. Eng. J.* **2019**, *364*, 89–101.

(16) Burdyny, T.; Smith, W. A. CO₂ reduction on gas-diffusion electrodes and why catalytic performance must be assessed at commercially-relevant conditions. *Energy Environ. Sci.* **2019**, *12*, 1442–1453.

(17) Rahbari, A.; Ramdin, M.; van den Broeke, L. J. P.; Vlugt, T. J. H. Combined Steam Reforming of Methane and Formic Acid To Produce Syngas with an Adjustable H₂:CO Ratio. *Ind. Eng. Chem. Res.* **2018**, *57*, 10663–10674.

(18) Agarwal, A. S.; Zhai, Y.; Hill, D.; Sridhar, N. The electrochemical reduction of carbon dioxide to formate/formic acid: Engineering and economic feasibility. *ChemSusChem* **2011**, *4*, 1301–1310.

(19) Jouny, M.; Luc, W.; Jiao, F. General Techno-Economic Analysis of CO₂ Electrolysis Systems. *Ind. Eng. Chem. Res.* **2018**, *57*, 2165–2177.

(20) Spurgeon, J. M.; Kumar, B. A comparative technoeconomic analysis of pathways for commercial electrochemical CO₂ reduction to liquid products. *Energy Environ. Sci.* **2018**, *11*, 1536–1551.

(21) Verma, S.; Kim, B.; Jhong, H.-R. M.; Ma, S.; Kenis, P. J. A.; Gross-Margin, A. Model for Defining Technoeconomic Benchmarks in the Electroreduction of CO₂. *ChemSusChem* **2016**, *9*, 1972–1979.

(22) Kertes, A. S.; King, C. J. Extraction chemistry of fermentation product carboxylic acids. *Biotechnol. Bioeng.* **1986**, *28*, 269–282.

(23) Murali, N.; Srinivas, K.; Ahring, B. K. Biochemical Production and Separation of Carboxylic Acids for Biorefinery Applications. *Fermentation* **2017**, *3*, No. 22.

(24) Kiss, A. A.; Lange, J.-P.; Schuur, B.; Brilman, D.; van der Ham, A.; Kersten, S. R. Separation technology-Making a difference in biorefineries. *Biomass Bioenergy* **2016**, *95*, 296–309.

(25) Greenblatt, J. B.; Miller, D. J.; Ager, J. W.; Houle, F. A.; Sharp, I. D. The Technical and Energetic Challenges of Separating (Photo)-Electrochemical Carbon Dioxide Reduction Products. *Joule* **2018**, *2*, 381–420.

(26) Ramdin, M.; Jamali, S. H.; van den Broeke, L. J.; Buijs, W.; Vlugt, T. J. CO₂ solubility in small carboxylic acids: Monte Carlo simulations and PC-SAFT modeling. *Fluid Phase Equilib.* **2018**, *458*, 1–8.

(27) Vermaas, D. A.; Wiegman, S.; Nagaki, T.; Smith, W. A. Ion transport mechanisms in bipolar membranes for (photo)-electrochemical water splitting. *Sustainable Energy Fuels* **2018**, *2*, 2006–2015.

(28) Vermaas, D. A.; Smith, W. A. Synergistic Electrochemical CO₂ Reduction and Water Oxidation with a Bipolar Membrane. *ACS Energy Lett.* **2016**, *1*, 1143–1148.

(29) Vermaas, D. A.; Sassenburg, M.; Smith, W. A. Photo-assisted water splitting with bipolar membrane induced pH gradients for practical solar fuel devices. *J. Mater. Chem. A* **2015**, *3*, 19556–19562.

(30) Strathmann, H.; Grabowski, A.; Eigenberger, G. Ion-Exchange Membranes in the Chemical Process Industry. *Ind. Eng. Chem. Res.* **2013**, *52*, 10364–10379.

(31) Ramdin, M.; Morrison, A. R. T.; de Groen, M.; van Haperen, R.; de Kler, R.; van den Broeke, L. J. P.; Trusler, J. P. M.; de Jong, W.; Vlugt, T. J. H. High Pressure Electrochemical Reduction of CO₂ to Cation Acid/Formate: A Comparison between Bipolar Membranes and Cation Exchange Membranes. *Ind. Eng. Chem. Res.* **2019**, *58*, 1834–1847.

(32) Li, Y. C.; Yan, Z.; Hitt, J.; Wycisk, R.; Pintauro, P. N.; Mallouk, T. E. Bipolar Membranes Inhibit Product Crossover in CO₂ Electrolysis Cells. *Adv. Sustainable Syst.* **2018**, *2*, No. 1700187.

(33) Li, Y. C.; Lee, G.; Yuan, T.; Wang, Y.; Nam, D.-H.; Wang, Z.; Garcia de Arquer, F. P.; Lum, Y.; Dinh, C.-T.; Voznyy, O.; Sargent, E. H. CO₂ Electroreduction from Carbonate Electrolyte. *ACS Energy Lett.* **2019**, *4*, 1427–1431.

(34) Pătru, A.; Binninger, T.; Pribyl, B.; Schmidt, T. J. Design Principles of Bipolar Electrochemical Co-Electrolysis Cells for Efficient Reduction of Carbon Dioxide from Gas Phase at Low Temperature. *J. Electrochem. Soc.* **2019**, *166*, F34–F43.

(35) Salvatore, D. A.; Weekes, D. M.; He, J.; Dettelbach, K. E.; Li, Y. C.; Mallouk, T. E.; Berlinguette, C. P. Electrolysis of Gaseous CO₂ to CO in a Flow Cell with a Bipolar Membrane. *ACS Energy Lett.* **2018**, *3*, 149–154.

(36) Li, Y. C.; Zhou, D.; Yan, Z.; Gonçalves, R. H.; Salvatore, D. A.; Berlinguette, C. P.; Mallouk, T. E. Electrolysis of CO₂ to Syngas in Bipolar Membrane-Based Electrochemical Cells. *ACS Energy Lett.* **2016**, *1*, 1149–1153.

(37) Ripatti, D. S.; Veltman, T. R.; Kanan, M. W. Carbon Monoxide Gas Diffusion Electrolysis that Produces Concentrated C₂ Products with High Single-Pass Conversion. *Joule* **2019**, *3*, 240–256.

(38) Xia, C.; Zhu, P.; Jiang, Q.; Pan, Y.; Liang, W.; Stavitsk, E.; Alshareef, H. N.; Wang, H. Continuous production of pure liquid fuel solutions via electrocatalytic CO₂ reduction using solid-electrolyte devices. *Nat. Energy* **2019**, *4*, 776–785.

(39) Mahmood, M. N.; Masheder, D.; Harty, C. J. Use of gas-diffusion electrodes for high-rate electrochemical reduction of carbon dioxide. I. Reduction at lead, indium- and tin-impregnated electrodes. *J. Appl. Electrochem.* **1987**, *17*, 1159–1170.

(40) Scialdone, O.; Galia, A.; Nero, G. L.; Proietto, F.; Sabatino, S.; Schiavo, B. Electrochemical reduction of carbon dioxide to formic acid at a tin cathode in divided and undivided cells: effect of carbon dioxide pressure and other operating parameters. *Electrochim. Acta* **2016**, *199*, 332–341.

(41) Ku, H. Notes on the use of propagation of error formulas. *J. Res. Natl. Bur. Stand., Sect. C* **1966**, *70C*, 263.

(42) Vassiliev, Y.; Bagotsky, V.; Osetrova, N.; Khazova, O.; Mayorova, N. Electroreduction of carbon dioxide. *J. Electroanal. Chem. Interfacial Electrochem.* **1985**, *189*, 271–294.

(43) Ryu, J.; Andersen, T. N.; Eyring, H. Electrode reduction kinetics of carbon dioxide in aqueous solution. *J. Phys. Chem. A* **1972**, *76*, 3278–3286.

(44) Paik, W.; Andersen, T.; Eyring, H. Kinetic studies of the electrolytic reduction of carbon dioxide on the mercury electrode. *Electrochim. Acta* **1969**, *14*, 1217–1232.

(45) Proietto, F.; Galia, A.; Scialdone, O. Electrochemical Conversion of CO₂ to HCOOH at Tin Cathode: Development of a Theoretical

Model and Comparison with Experimental Results. *ChemElectroChem* **2019**, *6*, 162–172.

(46) Li, H.; Oloman, C. Development of a continuous reactor for the electro-reduction of carbon dioxide to formate - Part 1: Process variables. *J. Appl. Electrochem.* **2006**, *36*, 1105–1115.

(47) Zhong, H.; Fujii, K.; Nakano, Y. Effect of KHCO₃ Concentration on Electrochemical Reduction of CO₂ on Copper Electrode. *J. Electrochem. Soc.* **2017**, *164*, F923–F927.

(48) Rumayor, M.; Dominguez-Ramos, A.; Irabien, A. Environmental and economic assessment of the formic acid electrochemical manufacture using carbon dioxide: Influence of the electrode lifetime. *Sustainable Prod. Consumption* **2019**, *18*, 72–82.

(49) Alvarez-Guerra, M.; Del Castillo, A.; Irabien, A. Continuous electrochemical reduction of carbon dioxide into formate using a tin cathode: Comparison with lead cathode. *Chem. Eng. Res. Des.* **2014**, *92*, 692–701.

(50) Proietto, F.; Schiavo, B.; Galia, A.; Scialdone, O. Electrochemical conversion of CO₂ to HCOOH at tin cathode in a pressurized undivided filter-press cell. *Electrochim. Acta* **2018**, *277*, 30–40.

(51) Kopljar, D.; Wagner, N.; Klemm, E. Transferring Electrochemical CO₂ Reduction from Semi-Batch into Continuous Operation Mode Using Gas Diffusion Electrodes. *Chem. Eng. Technol.* **2016**, *39*, 2042–2050.

(52) Del Castillo, A.; Alvarez-Guerra, M.; Solla-Gullón, J.; Sáez, A.; Montiel, V.; Irabien, A. Sn nanoparticles on gas diffusion electrodes: Synthesis, characterization and use for continuous CO₂ electro-reduction to formate. *J. CO₂ Util.* **2017**, *18*, 222–228.

(53) Irtem, E.; Andreu, T.; Parra, A.; Hernández-Alonso, M. D.; García-Rodríguez, S.; Riesco-García, J. M.; Penelas-Pérez, G.; Morante, J. R. Low-energy formate production from CO₂ electroreduction using electrodeposited tin on GDE. *J. Mater. Chem. A* **2016**, *4*, 13582–13588.

(54) Yang, H.; Kaczur, J. J.; Sajjad, S. D.; Masel, R. I. Electrochemical conversion of CO₂ to formic acid utilizing Sustainion membranes. *J. CO₂ Util.* **2017**, *20*, 208–217.

(55) Higgins, D.; Hahn, C.; Xiang, C.; Jaramillo, T. F.; Weber, A. Z. Gas-Diffusion Electrodes for Carbon Dioxide Reduction: A New Paradigm. *ACS Energy Lett.* **2019**, *4*, 317–324.

(56) Díaz-Sainz, G.; Alvarez-Guerra, M.; Solla-Gullón, J.; García-Cruz, L.; Montiel, V.; Irabien, A. Catalyst coated membrane electrodes for the gas phase CO₂ electroreduction to formate. *Catal. Today* **2018**, *1–7*.

(57) Lee, W.; Kim, Y. E.; Youn, M. H.; Jeong, S. K.; Park, K. T. Catholyte-Free Electrocatalytic CO₂ Reduction to Formate. *Angew. Chem., Int. Ed.* **2018**, *57*, 6883–6887.

(58) Gmehling, J., Ed. *Formic Acid–Water Azeotropic Data: Datasheet from 'Dortmund Data Bank (DDB)—Thermophysical Properties Edition 2014' in SpringerMaterials*, Springer-Verlag: Berlin, Heidelberg.

(59) Cusack, R.; Fremeaux, F.; Glatz, D.; Karr, A. A Fresh Look at Liquid–Liquid Extraction. *Chem. Eng.* **1991**.

(60) Gentry, J. C.; Solazzo, A. J. Recovery of Carboxylic Acids From Aqueous Streams. *Environ. Prog.* **1995**, *14*, 61–64.

(61) Glatz, D.; Parker, W. Enriching Liquid–Liquid Extraction. *Chem. Eng.* **2004**, *44–48*.

(62) Glatz, D.; Cross, B.; Lightfoot, T. Pilot Plant Testing for Liquid–liquid Extraction. *Chem. Eng. Prog.* **2018**, *24–30*.

(63) Sprakel, L.; Schuur, B. Solvent developments for liquid-liquid extraction of carboxylic acids in perspective. *Sep. Purif. Technol.* **2019**, *211*, 935–957.

(64) Reyhanitash, E.; Brouwer, T.; Kersten, S. R.; van der Ham, A.; Schuur, B. Liquid-liquid extraction-based process concepts for recovery of carboxylic acids from aqueous streams evaluated for dilute streams. *Chem. Eng. Res. Des.* **2018**, *137*, 510–533.

(65) Blahusiak, M.; Kiss, A. A.; Babic, K.; Kersten, S. R.; Bargeman, G.; Schuur, B. Insights into the selection and design of fluid separation processes. *Sep. Purif. Technol.* **2018**, *194*, 301–318.

(66) Brouwer, T.; Blahusiak, M.; Babic, K.; Schuur, B. Reactive extraction and recovery of levulinic acid, formic acid and furfural from aqueous solutions containing sulphuric acid. *Sep. Purif. Technol.* **2017**, *185*, 186–195.

(67) Müller, E.; Berger, R.; Blass, E.; Sluyts, D.; Pfennig, A. *Ullmann's Encyclopedia of Industrial Chemistry*; Wiley-VCH Verlag GmbH & Co. KGaA: Weinheim, Germany, 2008; pp 1–31.

(68) Robbins, L. A.; Cusack, R. *Perry's Chemical Engineer's Handbook*; Green, D., Perry, R., Eds.; McGraw-Hill: New York, 1999; Chapter 15, pp 15-1–15-47.

(69) Koch, J.; Shivel, G. Design Principles for Liquid–Liquid Extraction. *Chem. Eng. Prog.* **2015**, *111*, 22–30.

(70) Couper, J. R.; Penney, W. R.; Fair, J. R.; Walas, S. M. *Chemical Process Equipment*; Elsevier, 2012; pp 487–528.

(71) Cusack, R.; Glatz, D. Apply Liquid-Liquid Extraction to Today's Problems. *Chem. Eng.* **1996**, *103*, 1–16.

(72) Belova, V. V.; Zakhodyaeva, Y. A.; Voshkin, A. A. Extraction of carboxylic acids with neutral extractants. *Theor. Found. Chem. Eng.* **2017**, *51*, 786–794.

(73) Shah, V. H.; Pham, V.; Larsen, P.; Biswas, S.; Frank, T. Liquid-Liquid Extraction for Recovering Low Margin Chemicals: Thinking beyond the Partition Ratio. *Ind. Eng. Chem. Res.* **2016**, *55*, 1731–1739.

(74) Veith, H.; Voges, M.; Held, C.; Albert, J. Measuring and Predicting the Extraction Behavior of Biogenic Formic Acid in Biphasic Aqueous/Organic Reaction Mixtures. *ACS Omega* **2017**, *2*, 8982–8989.

(75) Aycock, D. F. Solvent Applications of 2-Methyltetrahydrofuran in Organometallic and Biphasic Reactions. *Org. Process Res. Dev.* **2007**, *11*, 156–159.

(76) Vian, M. A. In *Alternative Solvents for Natural Products Extraction*; Chemat, F., Vian, M. A., Eds.; Green Chemistry and Sustainable Technology; Springer Berlin Heidelberg: Berlin, Heidelberg, 2014.

(77) Hietala, J.; Vuori, A.; Johnsson, P.; Pollari, I.; Reutemann, W.; Kieczka, H. *Ullmann's of Encyclopedia of Industrial Chemistry*; Wiley-VCH Verlag GmbH & Co. KGaA: Weinheim, Germany, 2016; pp 1–22.

(78) Hangx, G. W. A.; Krooshof, G. J. P.; de Rijke, A. Process for the Separation of Formic Acid from Methyltetrahydrofuran. *WO2014184281A1*, 2014.

(79) Tirronen, E.; Laitinen, A.; Hietala, J. A Method and an Arrangement for Separating at Least One Carboxylic Acid and Furfural from a Dilute Aqueous Mixture Thereof. *US9073847B2*, 2013.

(80) Demesa, A. G.; Laari, A.; Tirronen, E.; Turunen, I. Comparison of solvents for the recovery of low-molecular carboxylic acids and furfural from aqueous solutions. *Chem. Eng. Res. Des.* **2015**, *93*, 531–540.

(81) Cai, W.; Zhu, S.; Piao, X. Extraction Equilibria of Formic and Acetic Acids from Aqueous Solution by Phosphate-Containing Extractants. *J. Chem. Eng. Data* **2001**, *46*, 1472–1475.

(82) Hu, L.; Adeyiga, A. A. Extraction of Formic Acid from Sodium Formate. *Ind. Eng. Chem. Res.* **1997**, *36*, 2375–2379.

(83) Morales, A. F.; Albet, J.; Kyuchoukov, G.; Malmay, G.; Molinier, J. Influence of Extractant (TBP and TOA), Diluent, and Modifier on Extraction Equilibrium of Monocarboxylic Acids. *J. Chem. Eng. Data* **2003**, *48*, 874–886.

(84) Sahin, S.; Bayazit, S. S.; Bilgin, M.; Inci, I. Investigation of Formic Acid Separation from Aqueous Solution by Reactive Extraction: Effects of Extractant and Diluent. *J. Chem. Eng. Data* **2010**, *55*, 1519–1522.

(85) Uslu, H. Reactive Extraction of Formic Acid by using Tri Octyl Amine (TOA). *Sep. Sci. Technol.* **2009**, *44*, 1784–1798.

(86) Wardell, J. M.; King, C. J. Solvent equilibria for extraction of carboxylic acids from water. *J. Chem. Eng. Data* **1978**, *23*, 144–148.

(87) Behroozi, M.; Vahedpour, M.; Shardi Manaheji, M. Separation of Formic Acid from Aqueous Solutions by Liquid Extraction Technique at Different Temperatures. *Phys. Chem. Res.* **2019**, *7*, 201–215.

(88) Bilgin, M.; Birman, I. Liquid phase equilibria of (water+formic acid+diethyl carbonate or diethyl malonate or diethyl fumarate) ternary systems at 298.15K and atmospheric pressure. *Fluid Phase Equilib.* **2011**, *302*, 249–253.

(89) Çehreli, S. Liquid-liquid equilibria of ternary systems (water +carboxylic acid+cumene) at 298.15K. *Fluid Phase Equilib.* **2006**, *248*, 24–28.

- (90) Çehreli, S.; Gündođdu, T. Phase equilibria of (water-carboxylic acid-diethyl maleate) ternary liquid systems at 298.15K. *Fluid Phase Equilib.* **2011**, *303*, 168–173.
- (91) Demirel, Ç.; Çehreli, S. Phase equilibrium of (water+formic or acetic acid+ethyl heptanoate) ternary liquid systems at different temperatures. *Fluid Phase Equilib.* **2013**, *356*, 71–77.
- (92) Ghanadzadeh Gilani, H.; Azadian, M. Tie-line data for water-formic acid-1-decanol ternary system at T=298.2, 303.2, 313.2, and 323.2K. *Thermochim. Acta* **2012**, *547*, 141–145.
- (93) Ghanadzadeh Gilani, H.; Asan, S. Liquid-liquid equilibrium data for systems containing of formic acid, water, and primary normal alcohols at T=298.2K. *Fluid Phase Equilib.* **2013**, *354*, 24–28.
- (94) Gündođdu, T.; Çehreli, S. Ternary liquid-liquid phase equilibria of (water-carboxylic acid-1-undecanol) systems at 298.15K. *Fluid Phase Equilib.* **2012**, *331*, 26–32.
- (95) İnce, E.; Kirbaslar, S. I.; Sahin, S. Liquid-Liquid Equilibria for Ternary Systems of Water + Formic Acid + Dibasic Esters. *J. Chem. Eng. Data* **2007**, *52*, 1889–1893.
- (96) İnce, E.; Lalikoglu, M.; Constantinescu, D. Liquid Phase Equilibria of the Water + Acetic Acid + Dimethyl Carbonate Ternary System at Several Temperatures. *J. Chem. Eng. Data* **2014**, *59*, 3353–3358.
- (97) Kumar, T. P.; Das, P. K. Solubility and tie-line data for water + formic acid + methyl isobutyl ketone ternary system at different temperatures. *Chem. Eng. Commun.* **2010**, *197*, 1163–1171.
- (98) Malmarmy, G.; Faizal, M.; Albet, J.; Molinier, J. Liquid-Liquid Equilibria of Acetic, Formic, and Oxalic Acids between Water and Tributyl Phosphate + Dodecane. *J. Chem. Eng. Data* **1997**, *42*, 985–987.
- (99) Özmen, D. Determination and correlation of liquid-liquid equilibria for the (water+carboxylic acid+dimethyl maleate) ternary systems at T=298.2K. *Fluid Phase Equilib.* **2008**, *269*, 12–18.
- (100) Senol, A. Liquid-Liquid Equilibria for Systems of (Water + Carboxylic Acid + Methylcyclohexanol) at 293.15 K: Modeling Considerations. *J. Chem. Eng. Data* **2004**, *49*, 1815–1820.
- (101) Senol, A. Liquid-Liquid Equilibria for Mixtures of (Water + Carboxylic Acid + 1-Octanol/Alamine 336) at 293.15 K. *J. Chem. Eng. Data* **2005**, *50*, 713–718.
- (102) Senol, A.; Bilgin, M.; Baslioglu, B.; Vakili-Nezhaad, G. Modeling phase equilibria of ternary systems (water + formic acid + ester or alcohol) through UNIFAC-original, SERLAS, NRTL, NRTL-modified, and three-suffix Margules: Parameter estimation using genetic algorithm. *Fluid Phase Equilib.* **2016**, *429*, 254–265.
- (103) Timedjehdine, M.; Hasseine, A.; Binous, H.; Bacha, O.; Attarakih, M. Liquid-liquid equilibrium data for water + formic acid + solvent (butyl acetate, ethyl acetate, and isoamyl alcohol) at T = 291.15 K. *Fluid Phase Equilib.* **2016**, *415*, 51–57.
- (104) Wang, Y.; Li, Y.; Li, Y.; Wang, J.; Li, Z.; Dai, Y. Extraction Equilibria of Monocarboxylic Acids with Trialkylphosphine Oxide. *J. Chem. Eng. Data* **2001**, *46*, 831–837.
- (105) Wisniewski, M.; Pierzchalska, M. Recovery of carboxylic acids C1-C3 with organophosphine oxide solvating extractants. *J. Chem. Technol. Biotechnol.* **2005**, *80*, 1425–1430.
- (106) Whitehead, K. E.; Geankoplis, C. J. Separation of Formic and Sulfuric Acids by Extraction. *Ind. Eng. Chem.* **1955**, *47*, 2114–2122.
- (107) Galaction, A.-I.; Kloetzer, L.; Cascaval, D. Influence of Solvent Polarity on the Mechanism and Efficiency of Formic Acid Reactive Extraction with Tri-n-Octylamine from Aqueous Solutions. *Chem. Eng. Technol.* **2011**, *34*, 1341–1346.
- (108) Hong, Y. K.; Hong, W. H.; Chang, Y. K. Effect of pH on the extraction characteristics of succinic and formic acids with Tri-n-octylamine dissolved in 1-octanol. *Biotechnol. Bioprocess Eng.* **2001**, *6*, 347–351.
- (109) Abdelkader, H. S.; Touhami, L.; Lakhdar, B. M.; Abdellah, K.; Toufik, G.; Fouzi, B. B. In *Study of the Effect of Some Parameters Governing the Recovery Process of Formic Acid from Its Aqueous Solution by Alcohols*, International Conference on Environmental, Biomedical and Biotechnology, Singapore, 2012; pp 205–210.
- (110) Eyal, A. M.; Canari, R. pH Dependence of Carboxylic and Mineral Acid Extraction by Amine-Based Extractants: Effects of pK_a, Amine Basicity, and Diluent Properties. *Ind. Eng. Chem. Res.* **1995**, *34*, 1789–1798.
- (111) Seyd, A. H.; Lanez, T.; Belfar, M. L. Modelling of yield and distribution coefficient in a liquid-liquid extraction: Effect of the concentration of ligand. *Asian J. Chem.* **2012**, *24*, 4511–4516.
- (112) Yang, S. T.; White, S. A.; Hsu, S. T. Extraction of carboxylic acids with tertiary and quaternary amines: effect of pH. *Ind. Eng. Chem. Res.* **1991**, *30*, 1335–1342.
- (113) Chanda, M.; O'Driscoll, K.; Rempel, G. Sorption of phenolics and carboxylic acids on polybenzimidazole. *React. Polym., Ion Exch., Sorbents* **1985**, *4*, 39–48.
- (114) Kunin, R.; Myers, R. J. The Anion Exchange Equilibria in an Anion Exchange Resin. *J. Am. Chem. Soc.* **1947**, *69*, 2874–2878.
- (115) Husson, S. M.; King, C. J. Multiple-Acid Equilibria in Adsorption of Carboxylic Acids from Dilute Aqueous Solution. *Ind. Eng. Chem. Res.* **1999**, *38*, 502–511.
- (116) Lin, X.; Xiong, L.; Huang, C.; Yang, X.; Guo, H.; Chen, X.; Chen, X. Sorption behavior and mechanism investigation of formic acid removal by sorption using an anion-exchange resin. *Desalin. Water Treat.* **2016**, *57*, 1–16.
- (117) Luo, G. S.; Wu, F. Y. Concentration of Formic Acid Solution by Electro-electrodialysis. *Sep. Sci. Technol.* **2000**, *35*, 2485–2496.
- (118) Luo, G.; Pan, S.; Liu, J. Use of the electrodialysis process to concentrate a formic acid solution. *Desalination* **2002**, *150*, 227–234.
- (119) Nagarale, R.; Gohil, G.; Shahi, V.; Trivedi, G.; Thampy, S.; Rangarajan, R. Studies on transport properties of short chain aliphatic carboxylicacids in electro-dialytic separation. *Desalination* **2005**, *171*, 195–204.
- (120) Jaime Ferrer, J. S.; Laborie, S.; Durand, G.; Rakib, M. Formic acid regeneration by electromembrane processes. *J. Membr. Sci.* **2006**, *280*, 509–516.
- (121) Jaime-Ferrer, J.; Couallier, E.; Viers, P.; Rakib, M. Two-compartment bipolar membrane electrodialysis for splitting of sodium formate into formic acid and sodium hydroxide: Modelling. *J. Membr. Sci.* **2009**, *328*, 75–80.
- (122) Jaime-Ferrer, J. S.; Couallier, E.; Viers, P.; Durand, G.; Rakib, M. Three-compartment bipolar membrane electrodialysis for splitting of sodium formate into formic acid and sodium hydroxide: Role of diffusion of molecular acid. *J. Membr. Sci.* **2008**, *325*, 528–536.
- (123) Zhang, N.; Peng, S.; Huang, C.; Xu, T.; Li, Y. Simultaneous regeneration of formic acid and carbonic acid from oxalate discharge by using electrodialysis with bipolar membranes (EDBM). *J. Membr. Sci.* **2008**, *309*, 56–63.
- (124) Lu, Y.; Luo, H.; Yang, K.; Liu, G.; Zhang, R.; Li, X.; Ye, B. Formic acid production using a microbial electrolysis desalination and chemical-production cell. *Bioresour. Technol.* **2017**, *243*, 118–125.
- (125) Selvaraj, H.; Aravind, P.; Sundaram, M. Four compartment mono selective electrodialysis for separation of sodium formate from industry wastewater. *Chem. Eng. J.* **2018**, *333*, 162–169.
- (126) Bui, M.; et al. Carbon capture and storage (CCS): The way forward. *Energy Environ. Sci.* **2018**, *11*, 1062–1176.
- (127) Ramdin, M.; de Loos, T. W.; Vlugt, T. J. State-of-the-Art of CO₂ Capture with Ionic Liquids. *Ind. Eng. Chem. Res.* **2012**, *51*, 8149–8177.
- (128) Bui, M.; et al. Carbon capture and storage (CCS): the way forward. *Energy Environ. Sci.* **2018**, *11*, 1062–1176.
- (129) Keith, D. W.; Holmes, G.; St. Angelo, D.; Heidel, K. A Process for Capturing CO₂ from the Atmosphere. *Joule* **2018**, *2*, 1573–1594.
- (130) House, K. Z.; Baclig, A. C.; Ranjan, M.; van Nierop, E. A.; Wilcox, J.; Herzog, H. J. Economic and energetic analysis of capturing CO₂ from ambient air. *Proc. Natl. Acad. Sci. U.S.A.* **2011**, *108*, 20428–20433.
- (131) Dinh, C.-t.; Li, Y. C.; Sargent, E. H. Boosting the Single-Pass Conversion for Renewable Chemical Electrosynthesis. *Joule* **2019**, *3*, 13–15.
- (132) Rubin, E. S.; Davison, J. E.; Herzog, H. J. The cost of CO₂ capture and storage. *Int. J. Greenhouse Gas Control* **2015**, *40*, 378–400.

(133) Bauer, F.; Persson, T.; Hulteberg, C.; Tamm, D. Biogas upgrading - technology overview, comparison and perspectives for the future. *Biofuels, Bioprod. Biorefin.* **2013**, *7*, 499–511.

(134) Feldhaus, P.; Vahlenkamp, T. *Transformation of Europe's Power System until 2050 Including Specific Considerations for Germany Electric Power and Natural Gas Practice*; McKinsey & Company, 2010.

(135) International Renewable Energy Agency. *Renewable Power Generation Costs in 2017*; IRENA, 2018.

(136) IEA. *Projected Costs of Generating Electricity*; OECD, 1998; p 215.

(137) IEA. *Levelized Cost and Levelized Avoided Cost of New Generation Resources in the Annual Energy Outlook 2019*; U.S. Energy Information Administration, Feb 1–12, 2019.

(138) Kost, C.; Schlegl, T.; Thomsen, J.; Nold, S.; Mayer, J.; Hartmann, N.; Senkpiel, C.; Philipps, S.; Lude, S.; Saad, N. *Levelized Cost of Electricity—Renewable Energy Technologies*; Fraunhofer Institute for Solar Energy Systems ISE, 2018.

(139) Schmidt, O.; Gambhir, A.; Staffell, I.; Hawkes, A.; Nelson, J.; Few, S. Future cost and performance of water electrolysis: An expert elicitation study. *Int. J. Hydrogen Energy* **2017**, *42*, 30470–30492.

(140) Dow-Mitsui. Dow and Mitsui form joint venture to build chlor-alkali plant. *Membr. Technol.* **2010**, *2010*, 8.

(141) Schmittinger, P.; Florkiewicz, T.; Curlin, L. C.; Lüke, B.; Scannell, R.; Navin, T.; Zelfel, E.; Bartsch, R. *Ullmann's Encyclopedia of Industrial Chemistry*; Wiley-VCH Verlag GmbH & Co. KGaA: Weinheim, Germany, 2011.

(142) European Commission. *Best Available Techniques (BAT) Reference Document for the Production of Chlor-alkali*, 2014; p 1030.

(143) Botte, G. G. Electrochemical Manufacturing in the Chemical Industry. *Interface Mag.* **2014**, *23*, 49–55.

(144) Glass, M.; Aigner, M.; Viell, J.; Jupke, A.; Mitsos, A. Liquid-liquid equilibrium of 2-methyltetrahydrofuran/water over wide temperature range: Measurements and rigorous regression. *Fluid Phase Equilib.* **2017**, *433*, 212–225.

(145) Todd, D. B. *Fermentation and Biochemical Engineering Handbook*, 2nd ed.; Elsevier, 2014; pp 225–238.

(146) Woods, D. R. *Rules of Thumb in Engineering Practice*; Wiley-VCH Verlag GmbH & Co. KGaA: Weinheim, Germany, 2007; pp 376–436.

(147) da Cunha, S.; Rangaiah, G. P.; Hidajat, K. Design, Optimization, and Retrofit of the Formic Acid Process II: Reactive Distillation and Reactive Dividing-Wall Column Retrofit. *Ind. Eng. Chem. Res.* **2018**, *57*, 14665–14679.

(148) da Cunha, S.; Rangaiah, G. P.; Hidajat, K. Design, Optimization, and Retrofit of the Formic Acid Process I: Base Case Design and Dividing-Wall Column Retrofit. *Ind. Eng. Chem. Res.* **2018**, *57*, 9554–9570.

(149) Chua, W.; da Cunha, S.; Rangaiah, G.; Hidajat, K. Design and optimization of Kemira-Leonard process for formic acid production. *Chem. Eng. Sci. X* **2019**, *2*, No. 100021.

(150) Verma, S.; Lu, S.; Kenis, P. J. A. Co-electrolysis of CO₂ and glycerol as a pathway to carbon chemicals with improved techno-economics due to low electricity consumption. *Nat. Energy* **2019**, *4*, 466–474.